

WP 1 Development of cross-border participative strategies in waste reduction

D.2.13.2 Conducted image analysis for the identification and monitoring of waste disposal sites

Published in July 2025 by Integrated waste reduction strategies and solutions in protected and Natura 2000 areas ©WASTEREDUCE Consortium, 2025

All rights reserved. Reproduction is authorized provided the source is acknowledged.

Funded by the European Union. Views and opinions expressed are however those of the author(s) only and do not necessarily reflect those of the European Union or EACEA. Neither the European Union nor the granting authority can be held responsible for them.

Disclaimer

The information, documentation and figures in this deliverable are written by the Integrated waste reduction strategies and solutions in protected and Natura 2000 areas - WASTEREDUCE project consortium under Subsidy contract NO: H93B23000040007 and do not necessarily reflect the views of the European Commission. The European Commission is not liable for any use that may be made of the information contained herein.

This deliverable contains original unpublished work except where clearly indicated otherwise. Acknowledgement of previously published material and of the work of others has been made through appropriate citation, quotation, or both. Reproduction is authorized provided the source is acknowledged.

Any dissemination of results reflects only the author's view, and the European Commission is not responsible for any use that may be made of the information it contains. The sole responsibility for the content of this publication lies with the authors.

Copyright message (only for interim reports)

This report, if not confidential, is not licensed

Document Information

Project ID	ITHR0200425	**Acronym**	WASTEREDUCE
2 - Green and resilient shared environment			
SO 2.2 - Protection of nature and biodiversity			
Project Full Title	Integrated waste reduction strategies and solutions in protected Natura 2000 areas		
Start Date	01/02/2024		
End Date	31/07/2026		
Duration (in months)	30		
Deliverable / Milestone	D 2.13.2 Conducted image analysis for the identification and monitoring of waste disposal sites		
Work Package	Development of cross-border participative strategies in waste reduction		
Date of Delivery	Contractual: 31/01/2025		Actual: 12/08/2025
Type	PDF Document		
Dissemination Level	CO = Confidential, only for members of the consortium including the Joint secretary and first level control		
Lead Beneficiary	University of Trieste, Department of Life Sciences		
	Valerio Tosti, Giovanni Bacaro	Organization:	Units
Reviewer(s)	All partners	Organization:	All partners
Document	This document, D.2.13.2, summarizes the methodologies and initial findings for waste detection using remote sensing. It explores the use of the Floating Debris Index (FDI) on satellite imagery for marine waste, finding it ineffective for small, scattered		

	debris due to low resolution. For land waste, a drone-based hyperspectral analysis was performed, revealing that while spectral signatures can differentiate waste, classification models failed due to a severe lack of training data. Ultimately, the study highlights critical limitations and trade-offs in remote sensing, concluding that current methods require significant refinement and that the project's waste database still relies on traditional field observations.

Document History

Version	Issue Date	Stage	Changes	Contributor
1	July 2025	Version 1	First full draft of the document	UNITS, ETRA, Natura Histrica
2	January 2026	Version 2	Final document	UNITS, ETRA, Natura Histrica
3				
4				

Table of Contents

Executive Summary 6

1. Introduction 8
1.1 Selected pilot sites 8
1.1.1. Akvatorij zapadne Istre 10
1.1.2. Ušće Raše 11
1.1.3. Ušće Mirne 12
1.1.4. Uvala Sakarun 13
1.1.5. “Grave e zone umide del Brenta” 14
1.2. Land waste detection 15
1.3. Application of Spectral indices 16
1.3.1. Floating Debris Index (FDI) 17
1.3.2. Normalized Difference Vegetation Index (NDVI) 18
1.3.3. Normalized Difference Water Index (NDWI) 18
1.3.4. Modified Bare Soil Index (MBI) 18
1.4. Hyperspectral images (HSI) 19

2. Applied Methodology 20
2.1. Used Satellite images 20
2.1.1. Floating marine debris detection 21
2.1.2. Land waste detection changes 21
2.2. Drone hyperspectral images and types of waste 22
2.2.1. Hyperspectral Classification Using Random Forest 24
2.2.2. Development of a Desktop Classification Application Using Spectral Angle Mapper 26

3. Results 28
3.1. Satellite image analysis 28
3.1.1. Floating Debris Index (FDI) 28
3.1.2. Land Waste Detection Through Change Analysis 34
3.2. Spectral Signature of Waste Types 35
3.2.1. Hyperspectral Classification Model Results 37
3.2.2. SAM Classification Application Results 40

4. Discussion and Conclusions 44

Reference List 46

Executive Summary

This document, D.2.13.2 “Conducted image analysis for the identification and monitoring of waste disposal sites”, outlines the methodologies and initial findings from a conducted image analysis for the identification and monitoring of waste disposal sites, serving as a critical step in the development of a standardized waste detection framework. The work presented explores the capabilities and limitations of using satellite and drone-based remote sensing across both marine and terrestrial environments. The study applied the Floating Debris Index (FDI) to Sentinel-2 satellite imagery to detect marine litter in several coastal pilot areas. While the FDI successfully isolated floating objects, its effectiveness for waste detection was severely limited by the imagery's 10x10 meter spatial resolution. This low resolution made it impossible to detect scattered marine debris, which is typically small and fragmented, while larger objects like boats were easily identified. This challenge was further compounded by the FDI’s inability to distinguish plastics from other floating materials such as seafoam and natural debris, ultimately preventing a robust, long-term statistical analysis of marine waste presence.

For land-based waste, a change detection analysis was performed using spectral indices on satellite imagery. This experiment aimed to link the spectral changes on a beach to the removal of waste after a cleanup event. However, the results were inconclusive, as the observed variations in the indices could not be definitively attributed to the absence of waste. Instead, other environmental factors like changes in soil humidity or tidal shifts appeared to be the primary drivers of these spectral fluctuations. This highlights the inherent difficulty of using such indices alone to reliably detect minor, scattered waste.

To address the limitations of satellite data, a hyperspectral drone survey was conducted to gather high-resolution imagery. This provided invaluable data for understanding the unique spectral signatures of different waste materials. The analysis confirmed that plastic color is a key factor in spectral identification, with polymer composition also playing a significant role. Based on this data, a Random Forest classification model was developed, but its performance was found to be unsatisfactory. The main reason for this was a critical lack of training data, as the waste classes had very few training pixels, leading to a high rate of overestimation and misclassification.

In conclusion, this study demonstrates that no single remote sensing methodology is a silver bullet for waste detection. While satellite imagery is useful for monitoring large-scale accumulations like illegal landfills, its resolution is inadequate for small, scattered waste. Drone imagery provides the necessary detail, but its limited spatial and temporal coverage, along with meteorological constraints, makes large-scale monitoring a logistical challenge. Given these uncertainties, the project’s official database of waste accumulation sites relies on traditional, reliable methods such as field observations. The work presented here, however, lays the essential groundwork for future development. To refine these methods, further analyses are planned to expand our training dataset, integrate both satellite and drone data,

and improve our classification models. The ultimate goal is to overcome the current limitations and establish a standardized, multi-faceted methodology for effective environmental waste monitoring.

1. Introduction

The accumulation of solid waste can release hazardous substances that contaminate the soil, making these sites significant sources of point-source pollution (Kah et al., 2012). However, the environmental impact extends beyond soil degradation. During rainfall or other precipitation events, these contaminants can be transported via surface runoff into adjacent water bodies such as rivers, lakes, and reservoirs (Marques, 2007; Baba et al., 2024; Harris, 1995). This process contributes to nonpoint source pollution, which poses serious risks to the quality of agricultural land and the safety of drinking water supplies. Given these environmental hazards, it is crucial to monitor and accurately map the spatial distribution of solid waste sites. Generating geo-referenced data facilitates informed environmental management, enhances risk assessment capabilities, and supports the development and implementation of effective pollution control strategies. The foundational work for this effort was conducted under Deliverable D 1.9.1, titled "Identifying, marking, and mapping locations in pilot-protected and Natura 2000 areas where waste is systematically accumulated". The primary aim of that action was to detect solid waste sites with high accuracy by proposing a novel deep learning model for mapping from very high-resolution remote sensing imagery. Building upon the insights and preliminary findings of D.1.9.1, the present document, D.2.13.2 “Conducted image analysis for the identification and monitoring of waste disposal sites”, focuses on the standardization of the methodologies used for conducting image analysis. The primary goal of this activity is to apply advanced remote sensing technologies and analytical methods to effectively detect and manage waste in ecologically sensitive regions, ensuring a repeatable and scientifically rigorous approach across the project’s selected pilot areas.

1.1. Selected Pilot Sites

The Natura 2000 network is the cornerstone of the European Union's biodiversity policy, representing a fundamental framework for environmental conservation across its member states. Its sites are designated under two principal legislative instruments: the Birds Directive (1979) and the Habitats Directive (1992), collectively known as the "Nature Directives." The overarching objective is to ensure the long-term conservation of Europe's most valuable and threatened species and habitats, thereby preventing biodiversity loss. This network serves as a key mechanism for fulfilling the EU's commitments under international agreements, such as the Bern Convention on the Conservation of European Wildlife and Natural Habitats, to which the EU is a contracting party. Consequently, Natura 2000 sites represent the EU Member States’ formal contribution to the Pan-European Emerald Network developed under this convention. The Birds Directive, in force since 1979, provides a comprehensive protection framework for all wild bird species naturally occurring in the EU. It mandates Member States to classify Special Protection Areas (SPAs) for 194 particularly threatened species listed in Annex I, as well as for all migratory birds, ensuring the preservation of key breeding, feeding, and resting sites. Building on this foundation, the Habitats Directive, adopted in 1992, expanded the scope of conservation to include a wide range of rare, endangered, or endemic natural habitats and non-avian species. It introduced the designation of Sites of Community Importance (SCIs) for the protection of 233 habitat types (Annex I) and over 900 species

(Annex II). Once adopted by the European Commission, SCIs must be designated by Member States as Special Areas of Conservation (SACs) within a six-year timeframe. Together, SPAs and SCIs/SACs form the Natura 2000 network. As of 2024, the network comprises over 27,000 sites, covering over 18% of the EU's terrestrial area and over 9% of its marine waters (European Commission, 2024). A defining characteristic of Natura 2000, unlike traditional nature reserves, is that it does not automatically exclude human activities. Instead, it promotes sustainable land and resource use, aiming to reconcile conservation objectives with economic, social, and cultural requirements, in line with the principle of sustainable development. This balanced approach is crucial for the effective management of such an extensive network. However, even within these protected areas, a significant challenge is posed by waste and pollution. Scientific literature and reports from institutions like the European Environment Agency (EEA) increasingly highlight how litter, particularly plastics, negatively impacts the very species and habitats that Natura 2000 aims to protect (EEA, 2019). The presence of waste can lead to species entanglement, ingestion of plastic particles, and habitat degradation, thereby undermining conservation efforts. This issue is particularly critical in coastal and riverine sites, which often act as accumulation zones for waste originating from both land- and sea-based sources. Therefore, a focused study on waste accumulation within these pilot sites is not only relevant but also essential for developing effective management strategies that support the long-term conservation goals of the Natura 2000 network. The subsequent sections of this report will provide detailed descriptions of the pilot areas selected by the project partners, which constitute the specific focus of this study. The table 1 below provides an overview of the official names of these pilot sites, their size, and their official classification according to the Natura 2000 nomenclature.

Site Code	Site Name	Country	Site Type	Official site
HR1000032	Akvatorij zapadne Istre	HR	Bird Directive	https://eunis.eea.europa.eu/sites/HR1000032
HR3000432	Ušće Raše	HR	Habitat Directive	https://eunis.eea.europa.eu/sites/HR3000432
HR3000433	Ušće Mirne	HR	Habitat Directive	https://eunis.eea.europa.eu/sites/HR3000433
HR3000069	Uvala Sakarun	HR	Habitat Directive	https://eunis.eea.europa.eu/sites/HR3000069
IT3260018	Grave e Zone umide della Brenta	IT	Habitat and Bird Directive	https://eunis.eea.europa.eu/sites/IT3260018

Table 1: A list of the selected pilot sites belonging to the Natura 2000 Network in Italy and Croatia, detailing their official names, extent, Natura 2000 classification, and the corresponding web addresses for more detailed information.

1.1.1 Akvatorij zapadne Istre

The Natura 2000 site "Akvatorij zapadne Istre" (site code HR1000032, Figure 1) is a crucial marine protected area located in the Jadranska Hrvatska region of Croatia. Established as a Special Protection Area (SPA) under the Birds Directive, this site has been officially recognized since July 2013 for its significant role in the conservation of avian biodiversity within the Mediterranean and Marine Mediterranean biogeographical regions. Encompassing an area of 155 square kilometers, with a dominant marine component of approximately 93%, the site's primary conservation objective is the protection of key bird populations. The area provides a vital habitat for six bird species listed in the Birds Directive's Annex I, including the Kingfisher (*Alcedo atthis*), Black-throated Diver (*Gavia arctica*), Red-throated Diver (*Gavia stellata*), the Mediterranean subspecies of Shag (*Phalacrocorax aristotelis desmarestii*), Common Tern (*Sterna hirundo*), and Sandwich Tern (*Sterna sandvicensis*). These species utilize the area for breeding, feeding, and as a resting point during migration, highlighting the

site's importance for the broader regional avian ecology. A key characteristic of "Akvatorij zapadne Istre" is its exclusive focus on avian conservation; notably, unlike many other Natura 2000 sites, it does not have any specific habitat types protected under the Habitats Directive (European Commission, 2023).



Figure 1: Overview of the Akvatorij zapadne Istre pilot site. The map illustrates the site's precise location and boundaries within the Jadranska Hrvatska region of Croatia. The base imagery for the map was sourced from Google Satellite, with processing and scale (1:450,000) managed through QGIS.

1.1.2 Ušće Raše

The Natura 2000 site "Ušće Raše" (site code HR3000432, Figure 2) is a significant conservation area located in the Jadranska Hrvatska region of Croatia. This site, with a surface area of 44.47 hectares—of which 86% is marine—has been protected under the Habitats Directive since its initial proposal as a Site of Community Importance (SCI) in July 2013 and subsequent confirmation in December 2014. Situated within the Mediterranean and Marine Mediterranean biogeographical regions, "Ušće Raše" is a crucial estuarine ecosystem, representing a vital interface where freshwater from the Raša River meets the Adriatic Sea. The site is designated for the protection of specific, rare species and two key habitat types. It safeguards one species listed in Annex II of the Habitats Directive: Painzza's Goby (*Knipowitschia panizzae*), a small fish species often found in brackish waters, which highlights the ecological importance of this unique transitional environment. The site also protects two distinct habitat types essential for biodiversity: sandbanks that are slightly covered by sea water all the time (habitat code 1110) and estuaries (habitat code 1130). Estuaries in particular, are among the most productive ecosystems on Earth, serving as critical nursery grounds for fish and providing essential habitats for a wide range of flora and fauna. The

conservation of these habitats is paramount for maintaining the ecological integrity of the Raša estuary and the broader coastal ecosystem of the region (European Commission, 2023).

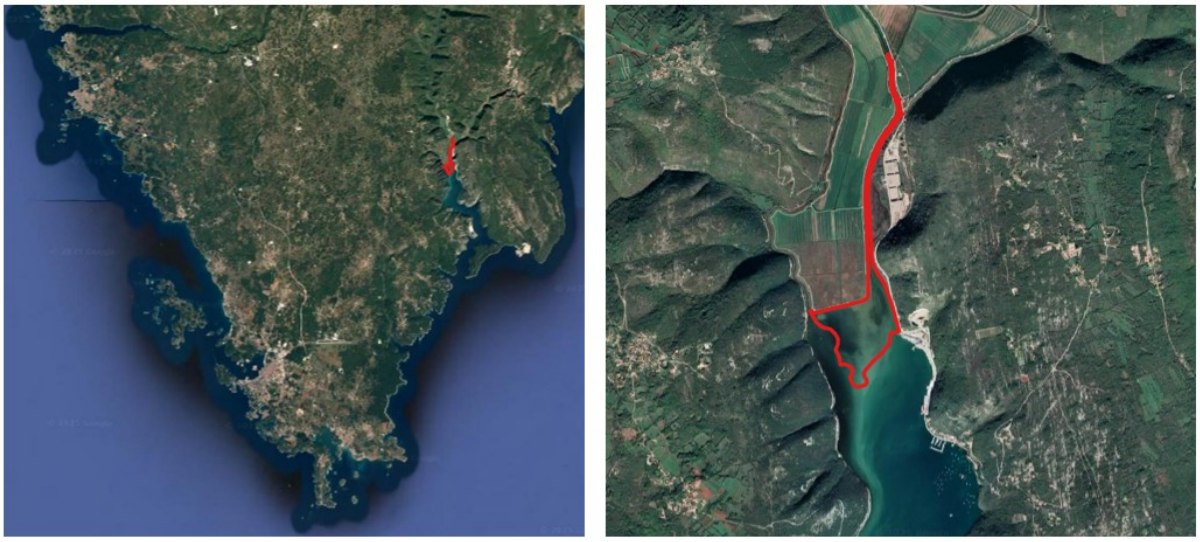


Figure 2: Overview of the Ušće Raše pilot site. The figure presents two maps to illustrate the site's boundaries: a broader regional map on the left (scale 1:300,000) and a more detailed, close-up map on the right (scale 1:37,500). The base imagery for both maps was sourced from Google Satellite, with processing and scale managed through QGIS.

1.1.3 Ušće Mirne

The Natura 2000 site "Ušće Mirne" (site code HR3000433, Figure 3) is a protected area located in the Jadranska Hrvatska region of Croatia. Covering a surface area of 115.34 hectares, with approximately 50% being marine, this site has been safeguarded under the Habitats Directive since it was first proposed as a Site of Community Importance (SCI) in July 2013 and subsequently confirmed in December 2014. Situated in the Mediterranean and Marine Mediterranean biogeographical regions, the site is notable for its estuarine ecosystem, where the Mirna River meets the sea. While "Ušće Mirne" is not designated for the protection of specific species, its ecological value is centered on the three distinct habitat types it protects. These include sandbanks that are slightly covered by seawater all the time (habitat code 1110) and estuaries (habitat code 1130), which are crucial as nursery areas for fish and crustaceans. Additionally, the site protects Mediterranean and thermo-Atlantic halophilous scrubs (habitat code 1420). This habitat type consists of salt-tolerant vegetation adapted to coastal and brackish environments, playing a vital role in stabilizing soil and supporting unique plant communities. The long-term conservation of these three habitats is essential for maintaining the biodiversity and natural processes of the Mirna River estuary and the surrounding coastal zone (European Commission, 2023).



Figure 3: Overview of the Ušće Mirne pilot site. The figure presents two maps to illustrate the site's boundaries: a broader regional map on the left (scale 1:250,000) and a more detailed, close-up map on the right (scale 1:35,000). The base imagery for both maps was sourced from Google Satellite, with processing and scale managed through QGIS.

1.1.4 Uvala Sakarun

The Natura 2000 site "Uvala Sakarun" (site code HR3000069, Figure 4) is a significant marine protected area in Croatia, located within the Marine Mediterranean biogeographical region. Encompassing an area of 438.54 hectares, which is entirely marine, the site has been safeguarded under the Habitats Directive since its proposal as a Site of Community Importance (SCI) in July 2013 and subsequent confirmation in December 2014. "Uvala Sakarun" is a key conservation area for two important habitat types that define the ecological character of the site. It is recognized for protecting *Posidonia* beds (*Posidonion oceanicae*) (habitat code 1120) and reefs (habitat code 1170). *Posidonia oceanica* is a species of seagrass endemic to the Mediterranean Sea that forms extensive underwater meadows, which are considered crucial ecosystems for the region. These meadows act as significant carbon sinks, produce oxygen, stabilize the seabed, and serve as vital nursery and breeding grounds for a diverse array of marine fauna (UNEP/MAP, 2011). Similarly, the reefs within the site provide complex habitats that support high biodiversity. Although the site does not protect any specific species under the Nature Directives, the conservation of these habitats is paramount for the overall health and productivity of the marine environment in the Northern Adriatic.



Figure 4: Overview of the Uvala Sakarun pilot site. The figure presents two maps to illustrate the site's boundaries: a broader regional map on the left (scale 1:500,000) and a more detailed, close-up map on the right (scale 1:60,000). The base imagery for both maps was sourced from Google Satellite, with processing and scale managed through QGIS.

1.1.5 “Grave e zone umide del Brenta”

The Natura 2000 site "Grave e Zone umide del Brenta" (site code IT3260018, Figure 5) is a significant conservation area located in the Veneto region of Italy, within the continental biogeographical region. Encompassing an extensive area of 3,848 hectares, this site has been under legal protection since September 1995 and is designated under both the Birds Directive and the Habitats Directive. This dual classification reflects its exceptional biodiversity, protecting both habitats and a wide array of species. The site was classified as a Special Protection Area (SPA) in August 2003 and later designated as a Special Area of Conservation (SAC) in July 2018. "Grave e Zone umide del Brenta" serves as a vital habitat for 55 species listed in the Nature Directives, highlighting its role as a biodiversity hotspot within the region. The protected species are remarkably diverse, including amphibians like the endemic Italian agile frog (*Rana latastei*), various bird species such as the Kingfisher (*Alcedo atthis*) and Grey Heron (*Ardea cinerea*), as well as significant populations of fishes, invertebrates, mammals, and reptiles. Furthermore, the site protects five important habitat types, which are crucial for maintaining the ecological integrity of the area. These include oligotrophic to mesotrophic standing waters, alpine rivers with ligneous vegetation, and alluvial forests with *Alnus glutinosa* and *Fraxinus excelsior*. Alluvial forests in particular, are a rare and important habitat type that supports a unique ecological community. The conservation of these habitats and species is paramount for the long-term ecological health of the Brenta river system and its surrounding wetlands (European Commission, 2023).



Figure 5: Overview of the Grave e Zone umide della Brenta pilot site. The figure presents two maps to illustrate the site's boundaries: a broader regional map on the left (scale 1:500,000) and a more detailed, close-up map on the right (scale 1:250,000). The base imagery for both maps was sourced from Google Satellite, with processing and scale managed through QGIS.

1.2. Land waste detection

Given the diverse nature of our pilot sites, which encompass both terrestrial and marine environments, the approach outlined in this deliverable follows a two-pronged strategy for remote sensing: one for land-based sites and another for marine areas. This section details the methodologies applicable to terrestrial landscapes, emphasizing that the selection of an appropriate remote sensing approach is not a one-size-fits-all solution. Instead, it requires a careful evaluation of technological capabilities against the specific characteristics and operational constraints of each pilot site. This foundational understanding of the available methods and their trade-offs is essential for creating a standardized, yet flexible, framework for waste detection and monitoring. Advancements in sensing technologies, remote sensing platforms, machine learning, and data fusion techniques have enhanced our capacity to identify, classify, and quantify waste materials across diverse terrestrial landscapes. These methods enable high-resolution spatial and temporal analysis of waste distribution, facilitating early intervention and informed decision-making. However, challenges persist, particularly in heterogeneous environments where waste is partially obscured, mixed with natural elements, or dispersed in fragmented forms. The effectiveness of waste detection from satellites is strongly dependent on the amount and volume of accumulated waste, and many studies today aim to detect wide waste depots such as landfills (Fraternali et al., 2024). The availability of very high-resolution (VHR) satellite imagery has significantly enhanced the capacity to monitor terrestrial environments. However, Fraternali et al. (2024) highlighted important trade-offs to consider: the selection of appropriate data sources must be guided by a careful evaluation of specific data requirements, as a clear trade-off exists between image resolution and associated costs. These costs extend beyond the acquisition phase to include data storage, transmission, and computational processing demands. A critical consideration in the design of waste detection systems is the optimization of four interrelated factors: spatial resolution,

temporal frequency (revisit time), cost-effectiveness, and the accuracy of the expected outcomes. Striking an appropriate balance among these parameters is essential to ensuring both the feasibility and efficiency of the monitoring solution. When the objective is to detect or track large-scale waste disposal sites, such as open landfills, moderate-resolution imagery acquired from satellites like Sentinel-2 or Landsat-8 is generally sufficient. These platforms offer data at little to no cost, with adequate spatial and spectral capabilities to identify surface anomalies such as elevated land surface temperatures or signs of vegetation stress commonly associated with unmanaged waste areas. Conversely, the detection of small and dispersed urban dumping sites, often concealed within densely built environments, requires much finer spatial detail. This level of resolution is typically achievable only through commercial satellites such as WorldView or Pléiades, which deliver sub-meter resolution imagery but at a significantly higher financial cost. The choice of such data sources must therefore be justified by the scale, sensitivity, and resolution demands of the application. Ultimately, the effectiveness of remote sensing-based waste detection strategies depends on aligning technological capabilities with the environmental context and operational constraints of the study area.

1.3. Application of Spectral indices

A fundamental approach to identifying and monitoring land-based waste sites (as well as marine areas) involves the use of spectral indices. These are mathematical formulas that combine the reflectance values from two or more spectral bands to highlight specific features of interest while suppressing others. This technique is particularly effective for detecting signs of environmental stress and changes in land cover that are commonly associated with waste accumulation. Remote sensing data captures the way different surfaces reflect light across various wavelengths of the electromagnetic spectrum. By leveraging these distinct spectral signatures, we can create indices that act as proxies for a range of environmental conditions. For instance, the presence of healthy vegetation, which strongly absorbs red light and reflects near-infrared light, can be quantified through a specific index. Conversely, the absence of vegetation or the presence of stressed vegetation, both of which are common at waste disposal sites, will produce a different spectral response, indicating a potential anomaly. Similarly, other combinations of spectral bands can be used to distinguish between different types of surfaces. Certain indices can highlight bare soil or built-up areas, which is useful for isolating waste from natural landscapes. The challenge in this approach lies in the potential for misclassification, as some waste materials may have spectral signatures similar to those of natural features. To mitigate this, a comprehensive strategy often involves the use of multiple indices and their integration with other data sources. This multi-index approach helps to reduce ambiguity, providing a more robust and reliable method for waste detection that is crucial for the standardization process across our diverse pilot sites. The following sub-sections will describe the spectral indices commonly used in the field of waste disposal identification, providing their mathematical formulation, a brief description, and their specific application for waste identification. For a more detailed description of these spectral indices, please refer to Deliverable D.1.9.1.

1.3.1. Floating Debris Index (FDI)

The Floating Debris Index (FDI) is a spectral index developed to detect floating materials on the surface of water bodies using satellite imagery. Introduced by Biermann et al. (2020), the FDI was designed to exploit the spectral characteristics of floating debris (plastics, seaweed, wood and spume) differentiating it from the water surface itself.
The FDI is computed using reflectance values from three key bands of the Sentinel-2 multispectral instrument (MSI): the second red edge band (RE2; 740 nm), the near-infrared band (NIR; 835 nm), and the shortwave infrared band (SWIR1; 1610 nm). The index uses the difference between the NIR (Rrs,NIR) and the baseline reflectance of NIR (R'rs,NIR), in which, the latter is derived from a linear interpolation between the NIR-flanking RE2 and SWIR1 bands:

$$\begin{aligned} FDI &= R_{rs,NIR} - R'_{rs,NIR} \\ R'_{rs,NIR} &= R_{rs,RE2} + (R_{rs,SWIR1} - R_{rs,RE2}) \times \frac{(\lambda_{NIR} - \lambda_{RED})}{(\lambda_{SWIR1} - \lambda_{RED})} \times 10 \end{aligned}$$

where R_{rs} refers to the reflectance value of the specified band, and *l* refers to the central value of the specified band's range in nm.

The floating debris typically shows elevated reflectance in the NIR region compared to the surrounding water, making it distinguishable by the index; it is particularly sensitive to anthropogenic materials, such as plastics, due to their distinctive spectral signatures, but it can detect all types of materials floating over the water surface (seaweed, timber, foam).
From a methodological standpoint, the FDI was initially optimized for the use of Sentinel-2 Level-1C imagery corrected to surface reflectance using ACOLITE (Atmospheric Correction for OLI 'lite'); ACOLITE is a processor specifically made to minimize the atmospheric interference for aquatic and coastal environments using satellite images. In contrast, Sen2Cor, the default atmospheric correction processor used to generate Sentinel-2 Level-2A products, is primarily designed for land applications and may perform inadequately over water surfaces. This can lead to unreliable retrievals of surface reflectance in marine environments, thereby potentially reducing the accuracy of indices like FDI.
Despite such limitations, some studies have explored the application of the FDI using Level-2A products processed with Sen2Cor (Topouzelis et al., 2019; Arachchilage et al., 2022). Also, Damayanti et al. (2022), in their study titled "Potential Marine Plastic Debris Detection using Sentinel-2 Multi-Spectral Instrument (MSI)", utilized Level-2A imagery to evaluate marine debris presence; while the study demonstrates the technical feasibility of using Sen2Cor-corrected data for floating debris detection, it also highlights the potential trade-offs in detection sensitivity and accuracy. Therefore, the FDI is most robust when applied to Sentinel-2 Level-1C data corrected with ACOLITE, but it remains adaptable with Level-2A data. However, it is important to consider the limitations of different atmospheric correction algorithms and their implications for accurate marine debris detection.

1.3.2. Normalized Difference Vegetation Index (NDVI)

The Normalized Difference Vegetation Index (NDVI) is a widely used remote sensing index designed to quantify vegetation vigor and biomass by exploiting the differential reflectance of vegetation in the red (665 nm) and near-infrared (835 nm) portions of the electromagnetic spectrum. NDVI values range from -1 to 1 and it is calculated as follows:

$$NDVI = \frac{(NIR - Red)}{NIR + Red}$$

where NIR refers to the reflectance in the near-infrared band and Red to the reflectance in the red band.

Healthy vegetation strongly absorbs visible light (especially red) for photosynthesis and reflects a large portion of near-infrared light; hence, NDVI effectively captures photosynthetic activity and vegetation density (Birky, 2001). In many studies the NDVI is used together with the land surface temperature (LST), and other vegetation indexes, to identify illegal landfills, mostly because of the possible stress induced by the accumulated waste to the vegetation in close proximity (Fraternali et al., 2024). Then, NDVI may be related to eventual presence of wastes on the environment.

1.3.3. Normalized Difference Water Index (NDWI)

The Normalized Difference Water Index (NDWI) is a spectral index designed to enhance the detection of surface water features using remote sensing data. It operates by maximizing the reflectance of water bodies while minimizing the reflectance from vegetation, built-up structures, and soil. The standard NDWI is defined by McFeeters (1996) as:

$$NDWI = \frac{GREEN - NIR}{GREEN + NIR}$$

where Green and NIR denote the reflectance values in the green (560 nm) and near-infrared (835 nm) spectral bands respectively.

Water bodies exhibit high reflectance in the green band and strong absorption in the NIR, making this formulation particularly effective for separating water from other land cover types. As a result, NDWI is useful for monitoring hydrological conditions, water stress in plants, and flood dynamics.

1.3.4. Modified Bare Soil Index (MBI)

The Modified Bare Soil Index (MBI) was introduced by Can Trong Nguyen *et al.* (2021) and it enhances the discrimination between non-vegetated surfaces and crop rotations. Nguyen *et al.* demonstrated that MBI outperforms other bare-soil indices (e.g. BSI, DBSI) in mapping fallow land, through a validation of their high accuracy through multi-regional assessment.
The MBI is calculated as follows:

$$MBI = \frac{SWIR1 - SWIR2 - NIR}{SWIR1 + SWIR2 + NIR} + f$$

where SWIR1 and SWIR2 refer to the reflectance in the short-wave infrared bands (respectively 1610 nm and 2200 nm), and NIR refers to the reflectance in the near-infrared band (835 nm).

The MBI values range from −0.5 to + 1.5, where bare soil is represented by positive values until the maximum. The choice of SWIR1 and SWIR2 stems from their sensitivity to soil moisture and their ability to differentiate surface materials based on water content and mineralogy. NIR, on the other hand, is used to filter out vegetative signals due to its strong reflectance in healthy vegetation. The addition of the constant factor (f) further normalizes the index, stabilizing the dynamic range and making it easier to apply threshold-based classification. Basically, the index uses the dissimilarities between bare soil, urban, and vegetation NIR, SWIR1 and SWIR2 bands as the basis to separate bare soil from other types of land cover.

1.4. Hyperspectral images (HSI)

Hyperspectral imaging (HSI) is a powerful remote sensing technique that captures image data across hundreds of contiguous spectral bands, extending beyond the visible range into the near-infrared and, sometimes, short-wave infrared regions. Each pixel in a hyperspectral image contains a complete reflectance spectrum, enabling the identification and classification of materials based on their unique spectral signatures (Chang, 2013). The integration of hyperspectral sensors with unmanned aerial vehicles (UAVs), commonly known as drones, has transformed environmental monitoring by enabling the collection of high-resolution spectral data at localized scales and flexible time intervals. In the context of environmental monitoring, drone-based HSI has been employed for a wide range of applications, including agricultural and natural vegetation health assessment, biodiversity mapping, invasive species detection, water quality monitoring, and soil characterization (Stuart et al., 2019; Laurin et al., 2014; Jay et al., 2006; Bansod et al., 2018; Anne et al., 2014). A particularly promising application of HSI in environmental science is the detection and monitoring of waste materials. Due to the high spectral sensitivity of hyperspectral sensors, it is possible to differentiate between natural and anthropogenic materials based on their spectral fingerprints. This capability has been increasingly explored in the identification of solid waste, including plastics, construction debris, and hazardous materials in terrestrial and aquatic environments (Mazanov et al., 2025; Bonifazi et al., 2021; Park et al., 2021). UAV-mounted hyperspectral systems allow for rapid, non-invasive surveys of illegal dumping sites, waste accumulation zones in rivers and coastal areas, and landfills, enabling both qualitative and quantitative assessments of waste distribution (Rajkumar et al., 2023).
Moreover, HSI can support efforts to classify waste by material type, aiding recycling and remediation strategies. Spectral libraries of common waste types, such as polyethylene, polystyrene, and other synthetic polymers, can be used in automated classification algorithms to map waste coverage with high precision (Kraśniewski et al., 2021; Bonifazi et al., 2021).

Nevertheless, several technical challenges remain, including accurate sensor calibration, geometric correction, data storage and processing constraints, and limited flight durations due to payload and energy restrictions. Addressing these challenges is an active area of research aimed at improving the operational efficiency and analytical accuracy of UAV-based hyperspectral systems in dynamic environmental conditions (Aasen et al., 2020).

2. Applied Methodology

2.1. Used Satellite Images

In this work, the methodologies for waste detection rely on satellite imagery as the primary source of data. Specifically, for the calculation of all spectral indices and analyses described in the following sub-sections, we have utilized images from the Sentinel-2 mission. This choice is driven by the mission's specific characteristics, which are particularly well-suited for environmental monitoring applications across both terrestrial and coastal areas. Sentinel-2 is a key component of the European Union's Copernicus Programme, providing high-resolution optical imagery for a wide range of land and sea observation services. The mission consists of a constellation of two identical satellites, Sentinel-2A and Sentinel-2B, which together offer a high revisit frequency of up to 5 days at the equator, and even more frequently at mid-latitudes. This temporal resolution is crucial for monitoring dynamic environmental processes and for ensuring data availability despite cloud cover. The satellites are equipped with the MultiSpectral Instrument (MSI), which captures images across 13 spectral bands, ranging from the visible and near-infrared (VNIR) to the short-wave infrared (SWIR) portions of the electromagnetic spectrum. These bands have varying spatial resolutions:

- 10-meter resolution: Four bands covering the visible (blue, green, red) and near-infrared (NIR) wavelengths. These are ideal for land cover classification, vegetation analysis, and general mapping.

- 20-meter resolution: Six bands in the "red edge" and short-wave infrared (SWIR) regions. The red edge bands are particularly useful for monitoring vegetation health and stress, while the SWIR bands are effective for discriminating between different types of soil, snow, ice, and for cloud and moisture detection.

- 60-meter resolution: Three bands dedicated to atmospheric correction and aerosol detection.

The combination of this high spatial resolution with a broad spectral range and frequent revisit time makes Sentinel-2 data a powerful and cost-effective tool for environmental monitoring tasks, including the detection of both land-based waste and floating marine debris. The characteristics of the Sentinel-2 mission thus provide the necessary foundation for the subsequent analyses detailed in this deliverable.

2.1.1. Floating marine debris detection

The detection of floating marine debris was approached using the Floating Debris Index (FDI), a specialized tool developed for marine and coastal environments. This methodology, while effective in some of our pilot areas, presented distinct limitations in others, revealing the crucial influence of local environmental conditions on remote sensing performance. The FDI was successfully applied to the Sakarun Bay and Istrian pilot areas. For these locations, a comprehensive time series of Sentinel-2 Level 2A images from 2024 was retrieved via Google Earth Engine (GEE). To ensure data quality, images with significant cloud cover were filtered out, using a 5% threshold for Sakarun Bay (yielding 34 images) and a slightly higher 15% threshold for the Istrian sites (32 images). Once the data was prepared, the FDI was calculated directly on each image within GEE. The resulting index, along with a corresponding RGB true-color image, was then imported into QGIS, allowing for a visual interpretation and validation of the debris objects detected by the index.
Conversely, the FDI proved to be an unsuitable method for river and lagoon environments due to a combination of elevated water turbidity and turbulent flow. Consequently, it was not applied to the Brenta, Ušće Raše, and Ušće Mirne pilot areas. In these environments, the increased turbidity and water motion can submerge floating debris, making it difficult for the index to produce accurate detections. This challenge aligns with findings from several studies (Biermann et al., 2020; Moshtaghi et al., 2021; Karakuş, 2023) which have highlighted these factors as key limitations to FDI performance in such dynamic, non-coastal settings. This distinction underscores the need to adapt remote sensing methodologies to the specific physical characteristics of each study site, a key principle of the standardization process outlined in this deliverable.

2.1.2. Land waste detection changes

To evaluate the potential of satellite imagery for detecting terrestrial waste, we conducted a targeted case study at Uvala Sakarun, a pilot area where a beach cleaning event on May 12, 2025, provided a unique opportunity. This event allowed us to gather remote sensing data of the same area both before (with accumulated waste) and after (without waste) the cleanup. Our goal was to test if satellite images could effectively identify the subtle changes resulting from the waste's removal, even with the inherent limitations of Sentinel-2's spatial resolution. We retrieved three Sentinel-2 Level 2A images of Uvala Sakarun from Google Earth Engine (GEE), with the extent precisely clipped to the beach area. The images were dated May 11 (the day before the cleanup), and May 14 and May 18 (the closest available dates after the cleanup). For each image, we calculated a suite of spectral indices. Following an initial correlation analysis, we selected three key indices for further statistical examination: the Normalized Difference Vegetation Index (NDVI), the Normalized Difference Water Index (NDWI), and the Modified Bare Soil Index (MBI). The MBI was considered particularly relevant for this study due to its ability to isolate bare soil from other materials, making it well-suited for quantifying changes related to the presence of waste on the ground. However, since MBI's performance can be influenced by soil humidity, we included the NDWI to assess any potential influence of soil water content on the MBI values. The indices calculated from the three dates were then processed in Python. We used the `*numpy*`, `*pandas*`, and `*tifffile*` libraries to extract a *DataFrame* for each image, representing the value of every single pixel. To account

for different lighting conditions between the dates, all pixel values were first normalized using a min-max approach:

$$\text{Normalized Value} = \frac{\text{ind.val - min.ind}}{\text{max.ind - min.ind}}$$

Here, *ind.val* is the pixel's original value, *min.ind* is the minimum value across all pixels in the image, and *max.ind* is the maximum value. Finally, a *t-test* was performed on the normalized pixel values using the `*scipy*` library to statistically evaluate the differences between the three images. The discussion of these results will follow in the next section, providing insight into the effectiveness of this methodology.

2.2. Drone hyperspectral images to identify types of waste

To complement the satellite-based analyses and provide high-resolution data for waste characterization, a drone-based survey was conducted over the beach of Uvala Sakarun on May 11, 2025, while waste was still present on site. The survey utilized a Matrice RTK 3000 drone equipped with a Cubert Ultris X20 hyperspectral camera. This advanced camera is a snapshot hyperspectral imager that acquires an entire datacube (spatial and spectral information) with a single image capture, eliminating motion artifacts and allowing for rapid, precise data collection. The Ultris X20 operates in the visible to near-infrared (VNIR) range, covering wavelengths from 350 nm to 1002 nm. It offers a high spectral resolution with 164 bands and captures images with a spatial resolution of 410 x 410 pixels. Acquisitions were taken over two distinct 10 x 10 meters plots established in different areas of the beach: one with small, fragmented waste, and the other with larger, clearly visible plastic bags (Figure 7). For each plot, two images were captured at different altitudes: 10 meters and 30 meters, resulting in pixel resolutions of 1.71 cm and 5.12 cm, respectively (Figure 6). This multi-scale approach was designed to assess the impact of spatial resolution on waste identification. Throughout the survey, extensive ground-level photographs of the waste were collected. These were later used to track and associate specific pixels in the drone images with the observed types of waste. However, due to the very small size of some items and the inherent difficulty in establishing pixel-level correspondence, only a portion of the waste could be accurately identified, particularly in the lower-resolution images captured at 30 meters. Due to the highly variable spectral responses of different waste materials, the identified items were grouped by color, a primary factor influencing their spectral behavior. The waste was categorized into five distinct color groups: 1) Black, 2) Yellow, 3) Blue, and 4) White wastes, plus a specific category for 5) Orange plastic bags. For larger waste items, it was also possible to define subclasses based on lighting conditions to account for variations in spectral signature caused by sun exposure. These subclasses were: - Bright (areas fully exposed to sunlight), - Mid-tone (partially exposed areas), and - Dark (shaded areas). Natural materials like rocks, *Posidonia* (seagrass), and wood were also grouped together to serve as a baseline for comparison.

All hyperspectral images were exported in TIFF format using *CubertExport* software and subsequently processed in Python. The spectral values for each waste group were extracted

using the `*numpy*`, `*pandas*`, and `*tifffile*` libraries, and the spectral signatures, the characteristic responses across all 164 bands from 350 to 1002 nm, were generated using `*pyplot*` from the `*matplotlib*` library. The analysis of these spectral signatures provides a crucial foundation for understanding how different waste types can be discriminated using hyperspectral data.

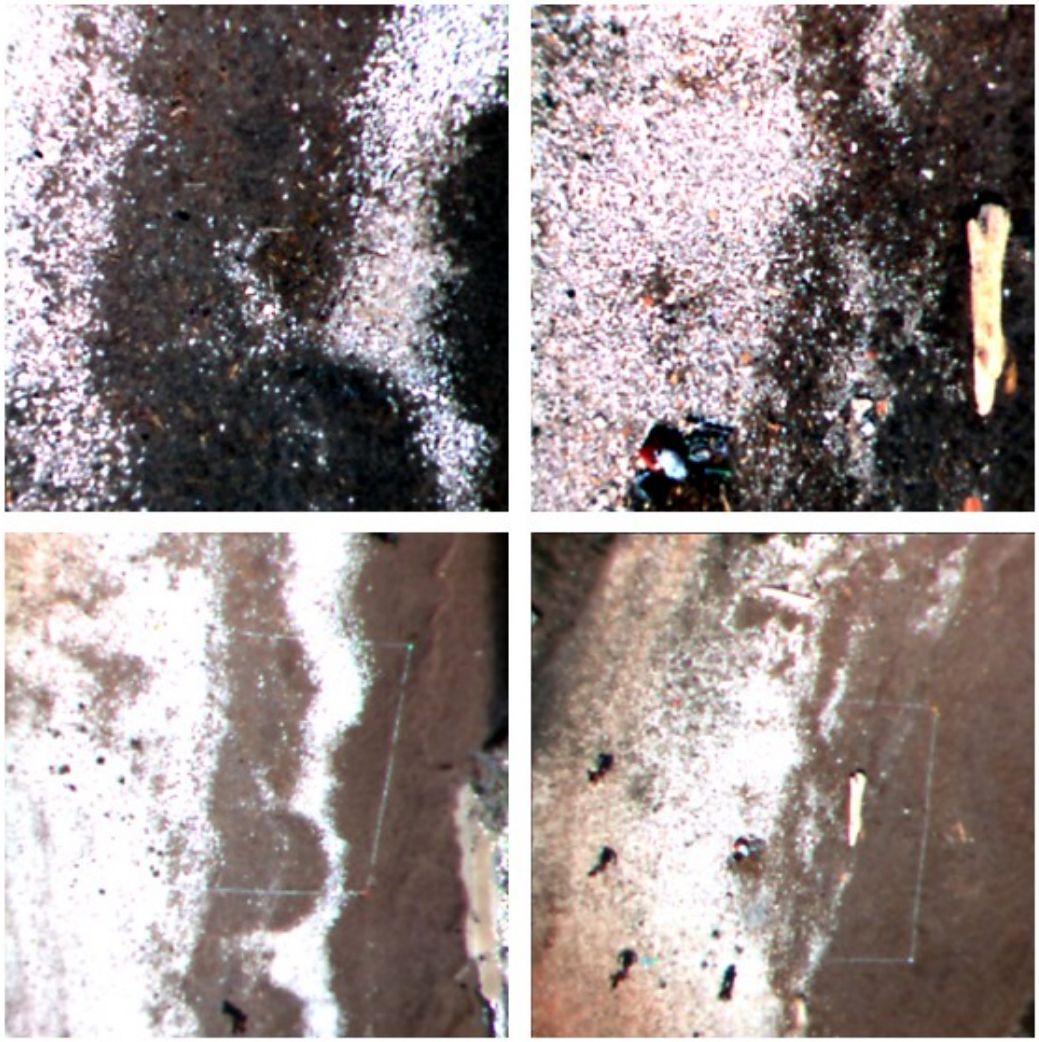


Figure 6: Hyperspectral drone imagery captured at two different altitudes over the study plots on Uvala Sakarun beach. The top images show Plot 1 (left) and Plot 2 (right) at a 10 m altitude, providing a high pixel resolution of 1.71 cm. The bottom images show the same plots at a 30 m altitude, with a coarser resolution of 5.12 cm.



Figure 7: On-field photographs taken during the drone survey at Uvala Sakarun beach. The left image shows Plot 1, characterized by small, fragmented waste, while the right image shows Plot 2, containing larger, clearly visible plastic bags.

2.2.1. Hyperspectral Classification Using Random Forest

To analyze the hyperspectral drone imagery, a supervised classification approach was used to distinguish between different waste materials and natural objects. This method involved training a machine learning model with the spectral signatures extracted from the images. The classification was performed using a Random Forest model, a powerful and widely used ensemble learning technique. The Random Forest algorithm works by constructing a multitude of decision trees during training and outputting the mode of the classes (for classification) or mean prediction (for regression) of the individual trees. This approach mitigates the risk of overfitting and enhances the model's accuracy and robustness, especially when dealing with high-dimensional datasets like hyperspectral imagery. For this analysis, the *RandomForestClassifier* from the '*sklearn'* library was utilized. To handle the high variability in the number of training pixels per class, the *class_weight* parameter was set to "balanced," which automatically adjusts the weight of each class inversely proportional to its frequency. The *n_estimators* parameter, which controls the number of trees in the forest, was set to 100 to ensure a stable and reliable prediction. The training data for the model was derived from the spectral signatures of both Plot 1 and Plot 2 images, with the data combined to maximize the number of training pixels available (Table 2). To account for the difference in image resolution, two separate classification models were developed: one for the 10-meter altitude images and another for the 30-meter images. This was necessary because the higher resolution of the 10-meter images allowed for the detection of small objects like bottle caps, which were not discernible in the lower-resolution 30-meter images. To optimize the model and reduce noise, a feature selection process was applied to the 164 hyperspectral bands. The least informative bands were removed: those in the ultraviolet spectrum (bands 1-14, 350-402 nm) and the portion affected by water absorption (bands 146-164, 930-1002 nm). From

the remaining bands, only one band every five was selected, resulting in a total of 25 bands spanning the 406-926 nm range for the model's training. The classes used for the models were carefully defined. Waste items were grouped by color, as this was the primary factor influencing their spectral signature. For larger items, subclasses were created to account for variations in lighting intensity (Bright, Mid-tone, and Dark). Natural materials, such as rocks and seagrass (*Posidonia*), were also included as distinct classes. The visualization of the classification results was carried out using the mcolors, ListedColormap, and Patch modules from the matplotlib library.

Table 2: this table shows the number of pixels assigned to each class for both the 10m and 30m resolution images, highlighting the different levels of detail and class distribution available at each scale. The classes include various types of waste grouped by color, as well as natural materials used for comparison.

10 m	
	n. of pixels
Black Wastes	14
Yellow Wastes	13
Blue Plastics	11
White Plastics	55
Orange Bag	20
Rocks	319
Posidonia	1582
Wood	350

30 m	
	n. of pixels
Black Wastes	6
Yellow Plastics	14
Blue Plastics	16
Red Plastics	16
White Plastics	28
Orange Bag	5
Rocks	1043
Posidonia	3441
Wood	189

2.2.2. Development of a Desktop Classification Application Using Spectral Angle Mapper

The hyperspectral drone imagery was also used, along with reference spectra data, to produce a desktop application designed to analyze hyperspectral images generating material classification maps using the Spectral Angle Mapper (SAM) algorithm.
The SAM is a physically based classification technique that evaluates the similarity between spectral signatures by treating them as vectors in a multidimensional feature space. The method computes the angle between the spectrum of each image pixel and a set of reference spectra, independently of illumination magnitude and albedo effects. Smaller angles indicate higher spectral similarity and therefore a greater probability that the pixel corresponds to a given material.
The spectral angle between each pixel vector and each reference vector is computed as follows:

$$\theta = \arccos\left(\frac{\mathbf{s}\cdot\mathbf{r}}{\|\mathbf{s}\|\|\mathbf{r}\|}\right)$$

where *s* is the pixel spectrum and *r* the reference spectrum.

The classification is performed by assigning all pixels to the class associated with the minimum spectral angle found, applying a threshold to reject unreliable matches. In this application a 0.05 threshold has been used, as it is the value ensuring a more conservative classification, and only the detected materials are retained for the final classification in order to reduce ambiguity. Due to its robustness to brightness variations and its limited sensitivity to sensor gain, SAM is widely adopted in hyperspectral remote sensing for material identification. The approach is particularly effective when accurate reference signatures are available and when spectral shape, rather than absolute reflectance, represents the main discriminative feature.
The spectral signature used as reference has been retrieved from the USGS spectral library (Kokaly et al., 2017); from all the data, only ASD field spectrometer measurements have been used, as they represent the best instrument to gather spectral data for remote sensing applications (Dugin et al., 2019). From all the ASD measurements, 33 artificial materials were selected including plastic, polyester, polystyrene and fiberglass with different physical characteristics such as color and other light interaction features (translucent, opaque, transparent). To include also natural materials in the reference spectra, the database was then integrated with the mean spectral value of dry and wet seagrass, rocks and woods, extracted from the drone images.
The classification application is intended for images acquired with hyperspectral sensors providing 163 contiguous spectral bands in the range 354–1002 nm, with a spectral sampling of 4 nm (one band every 4 nm). The application integrates several open-source Python libraries in order to manage image input/output, numerical processing, user interaction, and graphical visualization.
The graphical interaction with the user is handled through the *'tkinter'* library: at program start, an information window guides the user in selecting an appropriate image file and clarifies the spectral requirements of the dataset. The hyperspectral data is then loaded using the '*tifffile'* library as an array organized with dimensions (rows × columns × bands), then transformed into a tabular structure through the '*pandas'* library to facilitate inspection, export or integration with additional statistical routines.
Reference spectral signatures are stored in an external Excel file and imported using '*pandas'* library and they represent the endmembers used for classification. The core analytical procedure relies on the SAM algorithm, implemented using vectorized operations from *'numpy'*. Both image spectra and reference signatures are first normalized to unit length to remove the influence of illumination intensity.
The graphical output of the SAM classification is produced through the *'matplotlib'* library, displaying both the original image in a RGB visualization and the classification results to

facilitate the inspection and comparison between them. In addition to spatial visualization, the program also plots the spectral signatures of the materials identified in the scene, allowing direct comparison between reference spectra and detected materials. Each graphical output is displayed in an interactive window, where it is possible to zoom in specific areas, allowing a user-carried inspection of the results. All the outputs can also be saved as .png images.
Finally, the auxiliary function based on *'os'* and *'sys'* modules ensures that the database can be located both in development environments and in packaged executables eventually created with '*PyInstaller'*.

3. Results

3.1. Satellite image analysis

3.1.1. Floating Debris Index (FDI)

The application of the Floating Debris Index (FDI) to the coastal pilot areas for the entire 2024 provided critical insights into both the capabilities and the challenges of this methodology. While the index proved unsuitable for the turbid conditions of the Brenta River, Ušće Raše, and Ušće Mirne, it yielded clear and interpretable results for the other coastal sites. The analysis, however, highlighted the need for careful interpretation, especially in environments with high levels of human activity.

Uvala Sakarun

For the pilot area of Uvala Sakarun, an exhaustive review of all Sentinel-2 images from 2024 showed that no floating marine debris was detected over the coastal water surface. This finding is notable given the area's popularity. The FDI analysis successfully isolated floating objects on the water, but they were consistently identified as boats, either in transit or moored within the bay (Figure 8). The seasonal nature of these detections was particularly evident, with the first boat activity registered in June, followed by a marked increase throughout the peak summer months of July, August, and September. This outcome reveals a critical limitation related to the spatial resolution of the Sentinel-2 imagery, which operates at a 10x10 meter pixel size. Boats, being large objects, often occupy an entire pixel or a significant portion of it, making them clearly detectable by the FDI. In contrast, individual pieces of marine litter are typically small, fragmented, and scattered across the water surface. As a result, they occupy only a fraction of a single pixel, making them nearly invisible to this methodology. This distinction underscores a key challenge: the FDI, when applied to medium-resolution satellite data, is better suited for detecting large accumulations of floating debris rather than individual, scattered items. This serves as a vital lesson for refining the methodology for similar coastal environments in the future, suggesting that higher-resolution data or more advanced spectral analysis techniques may be necessary to address this limitation.

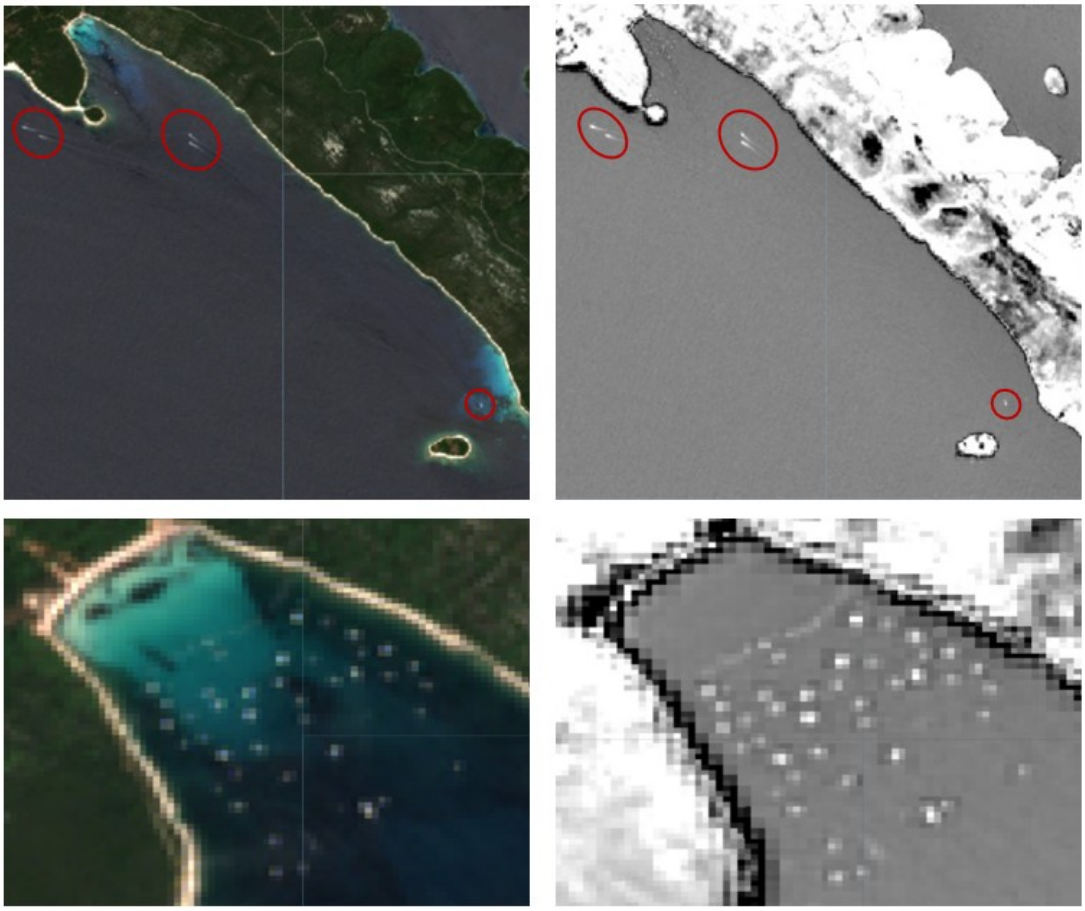


Figure 8: Satellite imagery of Uvala Sakarun illustrating the FDI detection results. The top row shows images from July 8, 2024, and the bottom row from August 7, 2024. In each pair, the RGB image (left) provides a baseline, while the Floating Debris Index (FDI) image (right) clearly isolates floating objects. The analysis consistently identified only moving and moored boats, with no marine litter detected on either date.

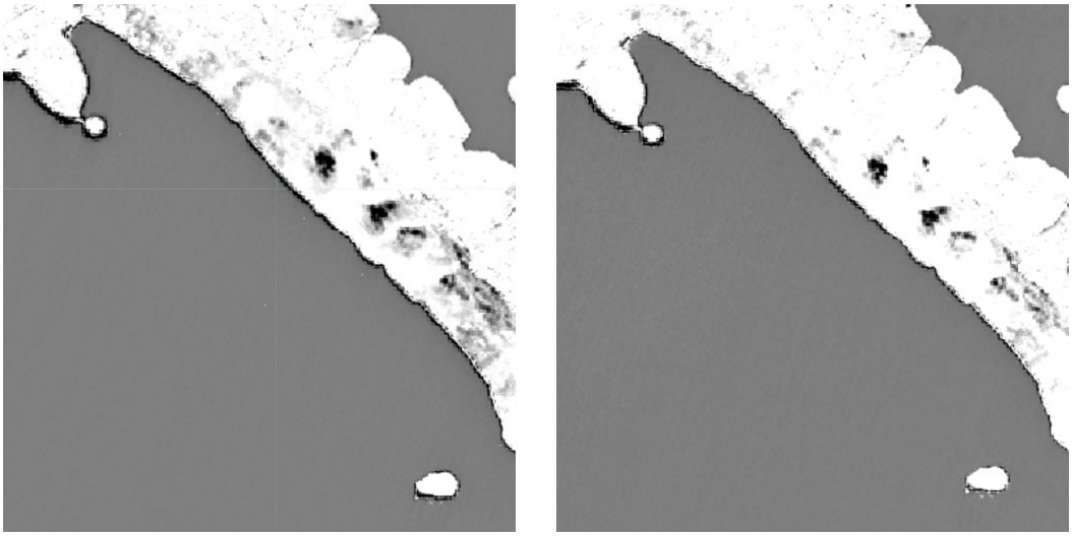


Figure 9: Satellite imagery processed with the Floating Debris Index (FDI) for Uvala Sakarun during the late autumn of 2024. The image from October 31 (left) and the image from November 15 (right) both confirm the absence of floating marine debris, in line with findings from the rest of the year.

Akvatorij zapadne Istre

The analysis of the Istrian coast provided a different outcome than Uvala Sakarun. Across the entire 2024 time series, the FDI did detect some floating debris. The detected objects displayed shapes and spectral characteristics typical of debris over the sea surface, confirming the index's ability to identify potential marine litter. However, the scarcity of these detections ultimately presented significant limitations that prevented us from conducting a robust statistical analysis.

I. Scarce presence of potential floating debris:

Throughout the year, the number of debris-related shapes found in the Istrian pilot areas was very low. Most of the available Sentinel-2 images showed a complete absence of debris, indicating that large-scale accumulations of litter were not a widespread or persistent issue in these coastal waters. This finding, while positive from an environmental perspective, meant that the dataset was insufficient to perform meaningful statistical comparisons or to track trends over time (Figure 10). The sparse and infrequent nature of the detections highlights a challenge inherent in remote sensing of dynamic and clean environments, the data may simply reflect the reality of minimal waste, rather than a failure of the detection method itself.

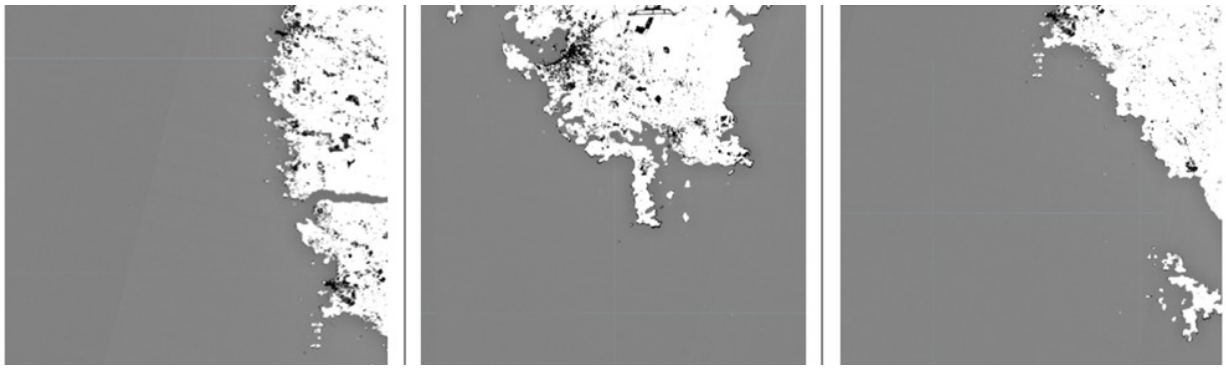


Figure 10: Satellite imagery of the Istrian coast processed with the Floating Debris Index (FDI) on April 29, 2024. This image illustrates a common finding from the analysis, where no floating marine debris was detected, highlighting the sparse nature of litter in this pilot area.

II. Difficulty distinguishing plastic debris from other materials:

A key challenge was the ambiguity of the FDI detections. While the index successfully identifies floating objects, it is not specifically designed to differentiate between types of materials. This makes it difficult to confirm the presence of plastic debris versus other substances like seafoam or natural sargassum mats. Our observations (Figure 11) revealed a high proportion of detected debris was also visible in the RGB imagery, suggesting it was likely seafoam, a naturally occurring, bright white substance easily distinguished in the visible spectrum. Conversely, plastic debris, especially transparent or pale-colored fragments, is more challenging to see in RGB images but is better detected by the FDI due to its spectral properties. This highlights a need for a multi-index approach or advanced classification models to effectively isolate plastic from other floating materials.

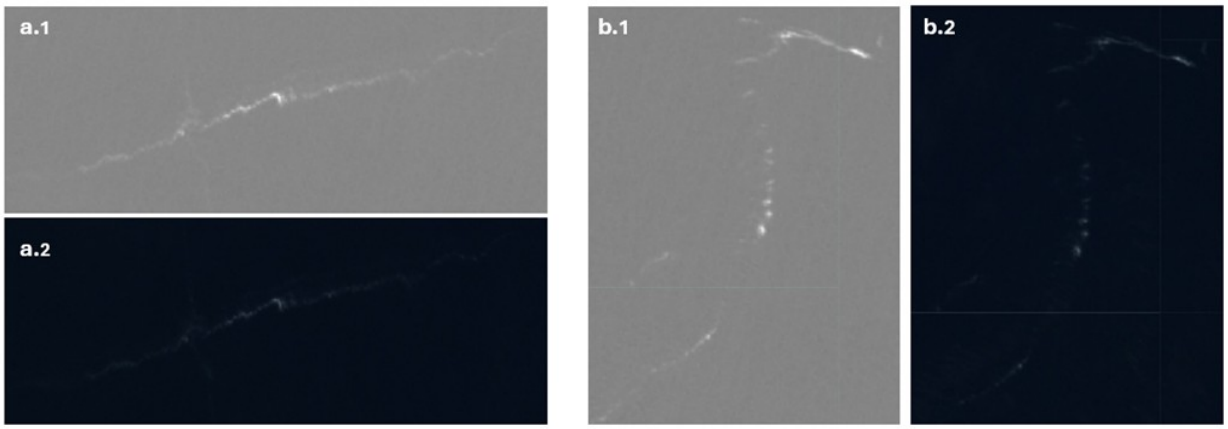


Figure 11: A comparison of potential seafoam debris detected by the FDI (a.1, b.1) and its corresponding appearance in RGB imagery (a.2, b.2) on July 28, 2024. The strong visibility in the RGB images suggests that the detected objects are likely seafoam rather than plastic debris.

III. Distance from the coast:

Most of the floating debris detected along the Istrian coast was located far offshore, making it very difficult to predict if and where it would eventually land (Figure 12). For the debris to pose a threat to coastal pilot areas, it must be transported to the shoreline. Predicting the pathway and destination of this debris requires additional data and modeling of sea currents and wind patterns. Therefore, while the FDI can identify the presence of debris in open waters, its utility for forecasting coastal accumulation is limited without a comprehensive oceanographic and meteorological analysis.

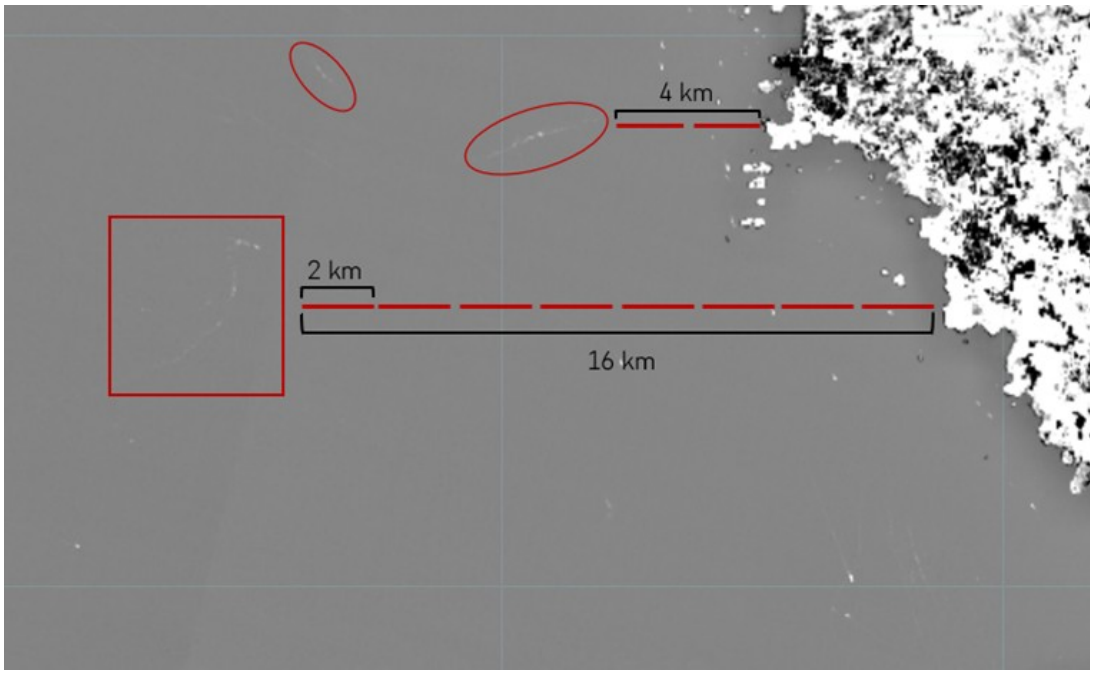


Figure 12: FDI-processed image of the Istrian coast on July 28, 2024, showing the detected debris patches and their considerable distance from the coastline.

IV. Disturbance from other elements:

Despite our efforts to filter images for cloud cover, the analysis was frequently hampered by residual cloud-covered sections, a problem exacerbated by the large spatial extent of the observed region (Figure 14). This issue was particularly prevalent during the autumn and winter months, but it also occurred in spring and summer, inevitably leading to a loss of information. Additionally, the FDI was prone to interference from other elements in the water, namely sea currents, seafoam, and boat traffic (Figure 13). Both seafoam and boats are also detected by the FDI, complicating the isolation of potential plastic debris. While boat activity is largely seasonal, coinciding with the tourist season, disturbances from sea currents and seafoam are sporadic and can occur at any time of the year.

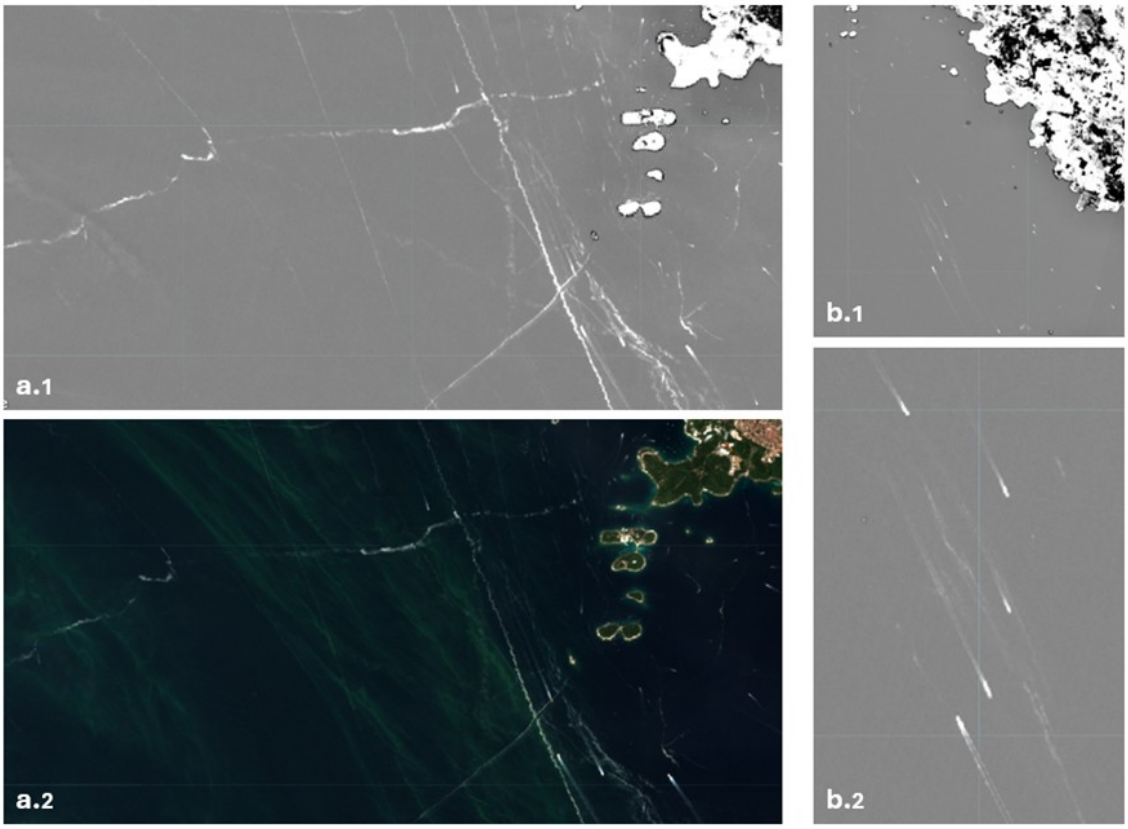


Figure 14: An example of disturbances affecting FDI analysis. Image (a.1) shows FDI detections on August 7, 2024, with corresponding RGB imagery (a.2) revealing the presence of boats, seafoam, and current patterns. The second example from August 12, 2024, shows a clear boat disturbance in both FDI (b.1) and RGB (b.2) images.

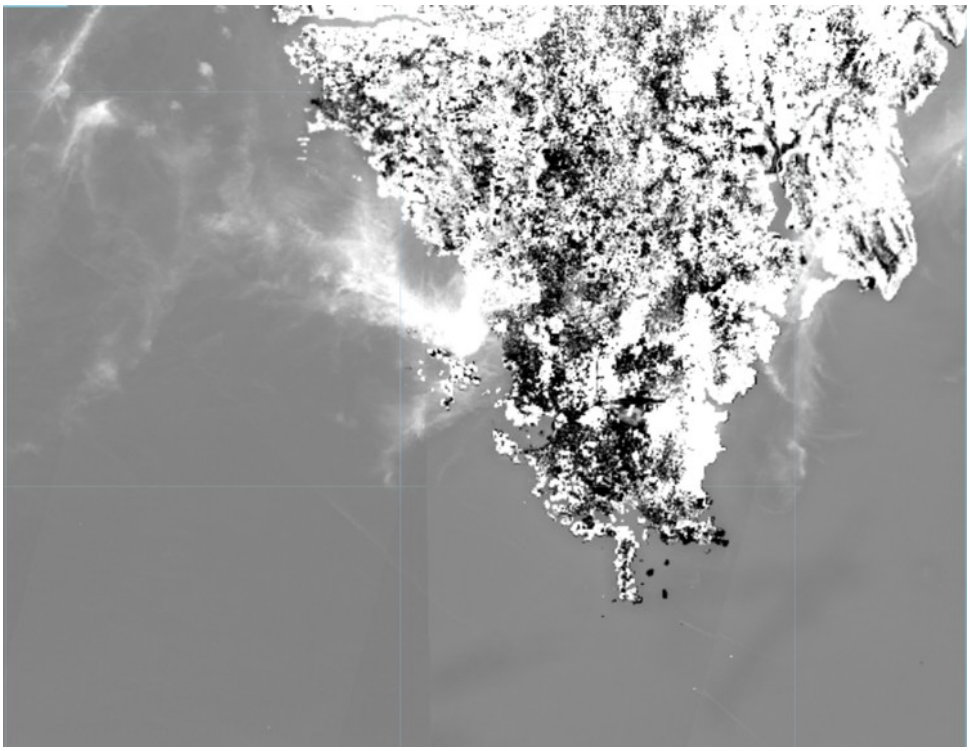


Figure 14: An FDI-processed image of the Istrian coast from August 22, 2024, illustrating the impact of partial cloud cover on data availability and analysis.

3.1.2. Land Waste Detection Through Change Analysis: Uvala Sakarun

The analysis of spectral indices at Uvala Sakarun aimed to evaluate if changes detected by satellite imagery could be definitively linked to the presence or absence of waste. Our methodology involved a change detection analysis using a t-test to compare three images: one from before the cleaning action (May 11) and two from after (May 14 and May 18). The results, however, revealed a complex and inconsistent pattern, making it difficult to attribute the observed changes solely to the removal of waste. As detailed in Table 3, the t-test showed a significant difference in the MBI and NDWI values between May 11 (with waste) and May 14 (without waste), a result that initially seemed promising. However, this interpretation was challenged by the subsequent comparison between May 14 and May 18, both dates from after the cleaning. A significant difference was again found for NDWI and MBI values, even though no waste was present on the beach on either date. This suggests that other environmental factors, such as changes in soil humidity, tidal movements, or natural shifts in the shoreline, may be the primary drivers of these spectral variations. Furthermore, the NDVI, which is typically sensitive to vegetation health, did not show a significant difference between the May 11 and May 14 images. This indicates that the small amount of waste on the beach did not significantly impact the vegetation, which would be expected given the beach's sandy composition.

The most striking inconsistencies were observed when comparing May 11 and May 18. This comparison showed significant differences in NDVI and NDWI, but not in MBI, completely contradicting the patterns seen in the other comparisons. The lack of a consistent signature across the different time intervals strongly suggests that factors other than the presence of waste are influencing the spectral values. Consequently, based on this single-site case study using Sentinel-2 imagery, we cannot conclude that spectral indices alone are sufficient for reliably detecting the presence of scattered waste on a beach environment. This finding underscores the need for a more controlled experimental design or the use of higher-resolution data to isolate the spectral signature of waste from other natural variables.

Table 3: Results of the t-test comparing NDVI, NDWI, and MBI values from three different dates (May 11, 14, and 18, 2025) on Uvala Sakarun beach. The table shows which comparisons yielded a statistically significant difference ($p < 0.05$) between the index values.

	11th vs 14th		11th vs 18th		14th vs 18th	
	t-statistic	p-value	t-statistic	p-value	t-statistic	p-value
NDVI	0,548155	0,584102	4,023187	7,77394E-05	3,411918	0,000759
NDWI	-3,583601	0,000412	-6,152119	3,39267E-09	-2,698547	0,007470
MBI	-3,730205	0,000239	-1,663489	0,097531	2,025099	0,043977

3.2. Spectral Signature of Waste Types from Hyperspectral Imagery

Using high-resolution hyperspectral images of Uvala Sakarun beach, combined with on-field photographs, we extracted the unique spectral signatures for various types of waste materials present on the site. Most of these materials consisted of plastics, including bags, nets, caps, tubes, and smaller fragments. This detailed analysis provides crucial insights into how different waste types interact with light across the electromagnetic spectrum. The results showed a high degree of consistency within each plastic color group, with one notable exception: the black waste category. The two elements classified as black had substantially different material compositions, which was clearly reflected in their distinct spectral signatures. This finding confirms that plastic color is a key factor in spectral identification, primarily influencing the visible spectrum (Balsi et al., 2018). However, other intrinsic properties of the material, particularly its polymer composition, also play a significant role. These properties are more discernible in the near-infrared (NIR) and shortwave infrared (SWIR) regions, where different polymers exhibit unique absorption features (Zhou et al., 2022; Olyaei et al., 2024). The spectral signatures derived from this analysis are invaluable for building accurate classification models. By understanding the specific spectral "fingerprints" of different waste types, we can train algorithms to identify and differentiate between them with greater precision. This detailed characterization is a fundamental step toward developing robust methodologies for automated waste detection and classification from remote sensing data.

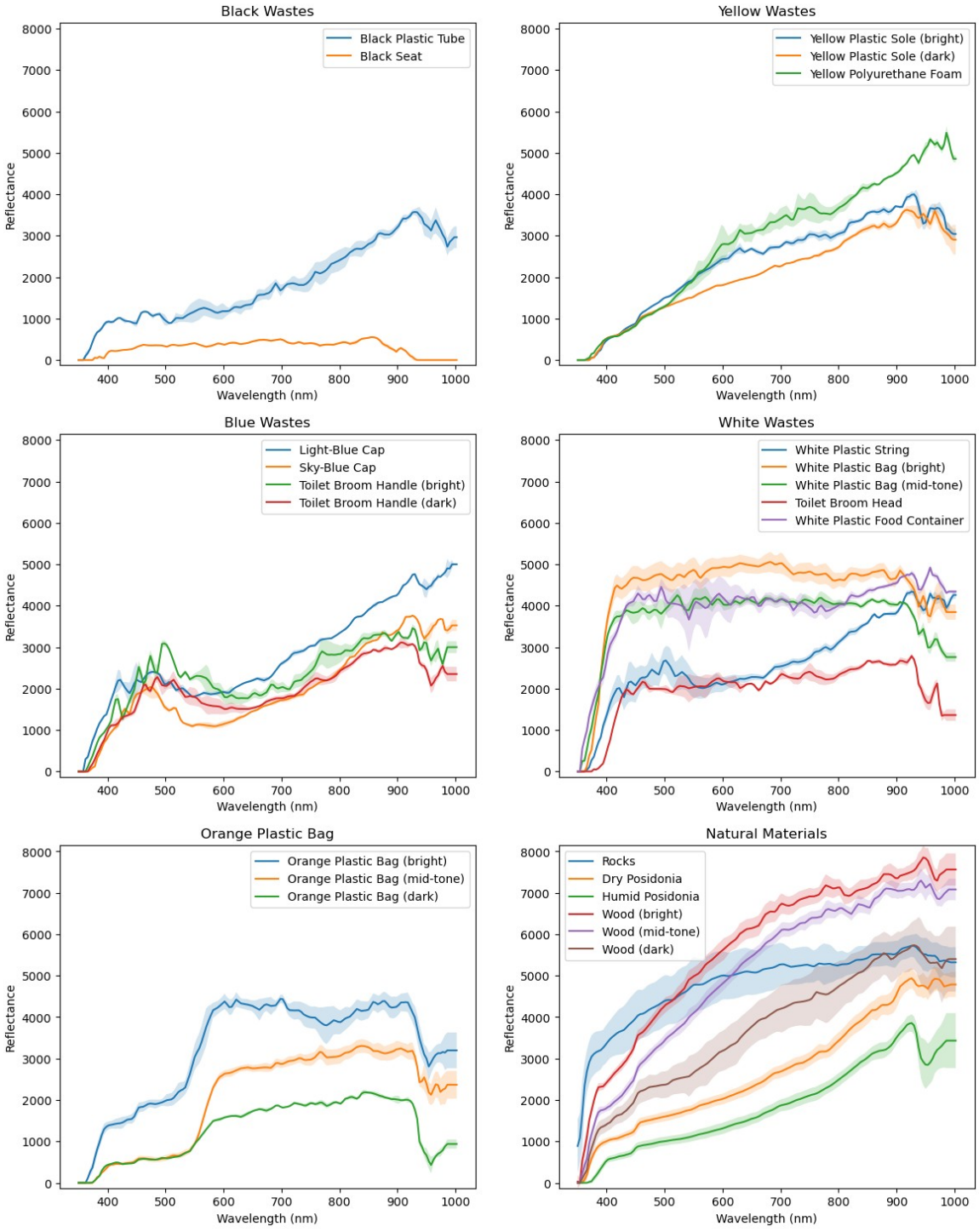


Figure 15: Spectral signatures of various waste and natural materials found on Uvala Sakarun beach. The chart displays the spectral response (reflectance) across 164 bands, ranging from 350 nm to 1002 nm, for each categorized material.

3.2.1. Hyperspectral Classification Model Results

Fig. 16 and 17 shows the output of the models, where the original RGB image is shown next to the classification. Both models were not satisfying, even if using 10 m images the performance was better compared to 30 m.
Even if the accuracy for Posidonia, rocks and wood is acceptable, the classification seems to have problems in overestimating waste, mainly concerning the white plastics where there should be rocks, but also for orange plastics in some small portions of Posidonia. At 30 m instead, there is a high overestimation of blue, yellow and red plastics and the overall accuracy is significantly reduced.
The main problem is probably the low amount of training pixels for waste classes, ranging from 11 to 55 for the 10 m images, and from 5 to 28 for the 30 m images (Table 2). The identification of pixels for natural materials instead was drastically easier, and the number of training pixels was significantly higher than those for waste; in fact, the model seems to better recognize those classes related to rocks, Posidonia and wood.
However, the large size wastes in plot 2, such as the white and orange plastic bag and the black seat, are well identified by the model at 10 m, while at 30 m they are still detected, but white plastic is classified as red. Even the large trunks present in plot 2 image at 30 m are well detected and classified. This suggests that the dimensions of the objects are another important factor influencing waste detection in the environment, but also that at different acquisition height and image resolution the spectral signal may change.

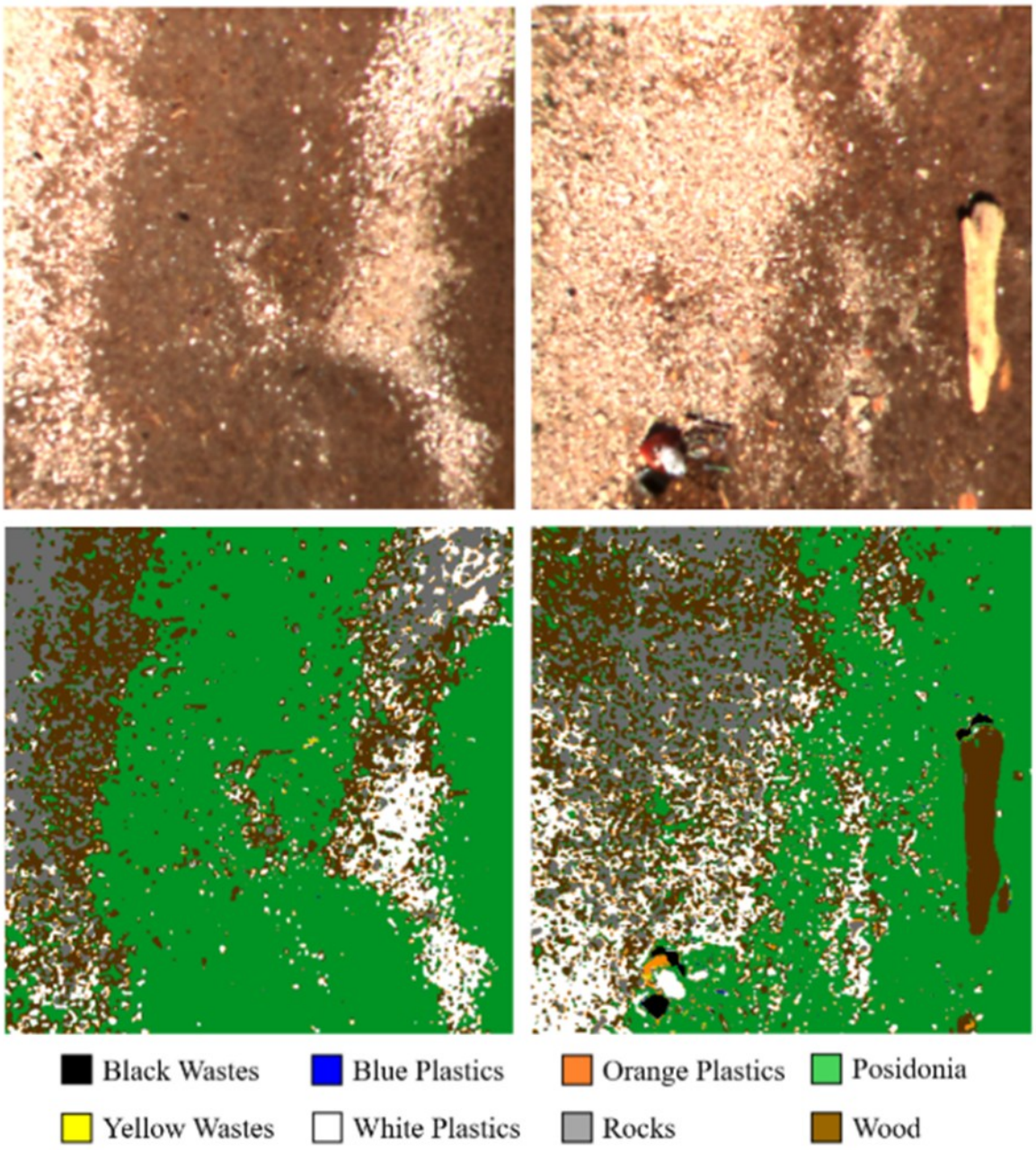


Figure 16: A comparison of the original RGB drone images (top) with the classification model's output (bottom) for Plot 1 (left) and Plot 2 (right) at 10 m of height and 1,71 cm of spatial resolution.

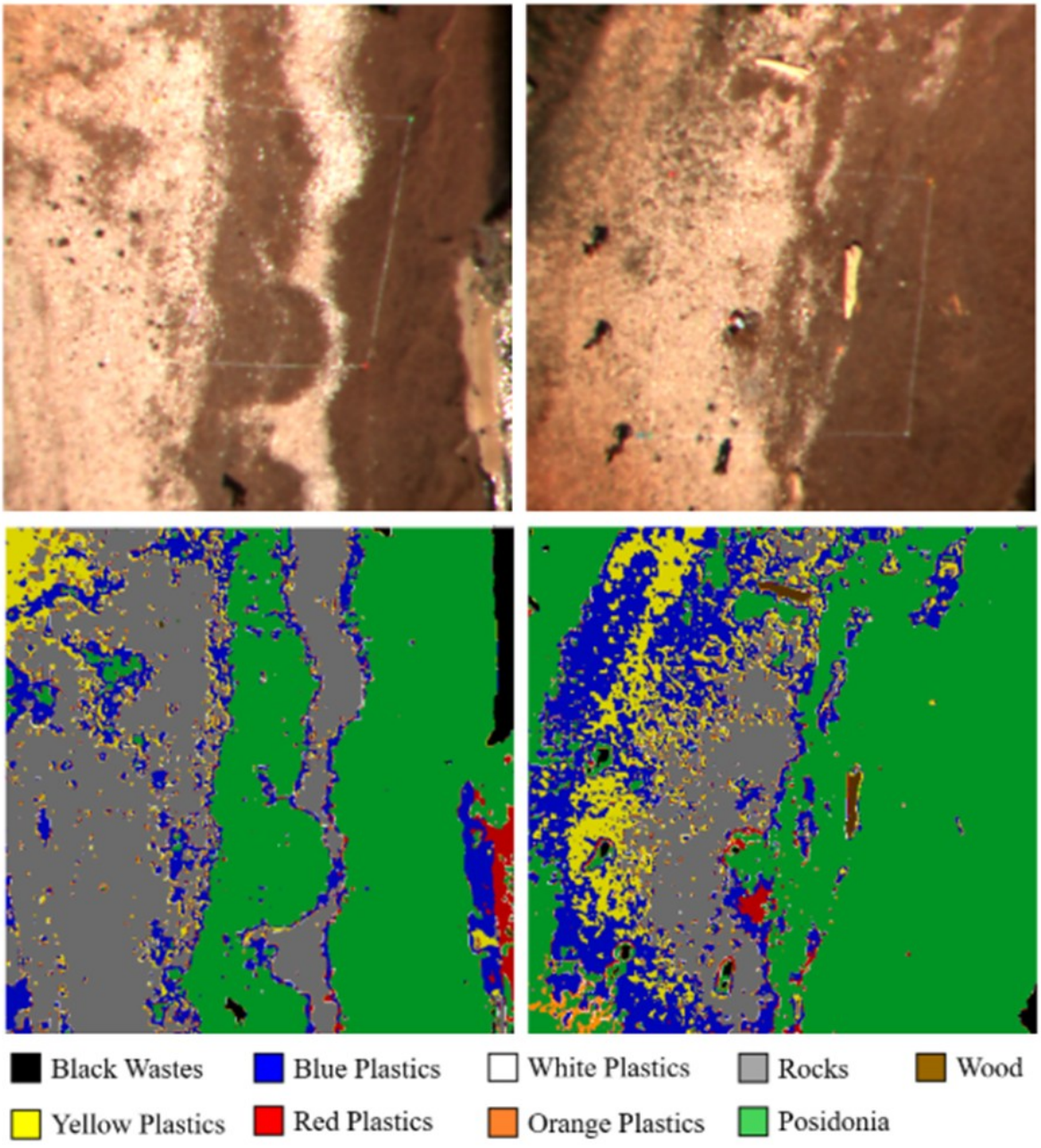


Figure 17: Original RGB images from the drone (top) compared with the model classification (bottom) of plot 1 (left) and plot 2 (right) at 30 m of height and 5,12 cm of spatial resolution.

3.2.2. SAM Classification Application Results

The classification application was tested on the hyperspectral images acquired in Sakarun Bay in order to evaluate its performance on datasets with different spatial resolutions. For both Plot 1 and Plot 2, three images were analyzed: (1) data collected at a flight height of 10 m, corresponding to a spatial resolution of 1.71 cm (Fig. 18); (2) data acquired at 20 m, with a spatial resolution of 3.42 cm (Fig. 19); and (3) data collected at 30 m, providing a spatial resolution of 5.12 cm (Fig. 20).
The classification results obtained from the images with 1.71 cm spatial resolution appear overall accurate for Plot 2, where the accumulated waste is clearly identified. In this area, the detected materials correspond to High-Density Polyethylene (HDPE) for the white plastic bag and Fiberglass for the black seat. Although the material types were correctly recognized, some limitations emerged in the identification of the correct color. This issue may be related to the reference spectral library, which included only four types of fiberglass and did not contain any spectra for black fiberglass. Similarly, the white plastic bag was classified as grey HDPE, likely due to shading effects; this effect is no longer observed in the image acquired at 20 m (Fig. 19), where the object is correctly classified as white HDPE.
In Plot 1, the waste was more fragmented and characterized by smaller object dimensions, which negatively affected the classification performance. In this case, some rocks were misclassified as Polyethylene Terephthalate (PETE) and Vinyl. The areas identified as Vinyl correspond to zones where rocks are larger or more densely clustered, resulting in increased surface brightness and reflectivity, which may explain the observed misclassification.
The analysis of the lower resolution images did not allow reliable identification of waste (Fig. 19-20), with the only exception being the previously mentioned white plastic bag in Plot 2 at 20 m flight height and 3.42 cm spatial resolution (Fig. 19). These results suggest that both the physical dimensions of waste and the spatial resolution of the imagery represent crucial factors influencing the capability to detect and correctly classify waste materials.

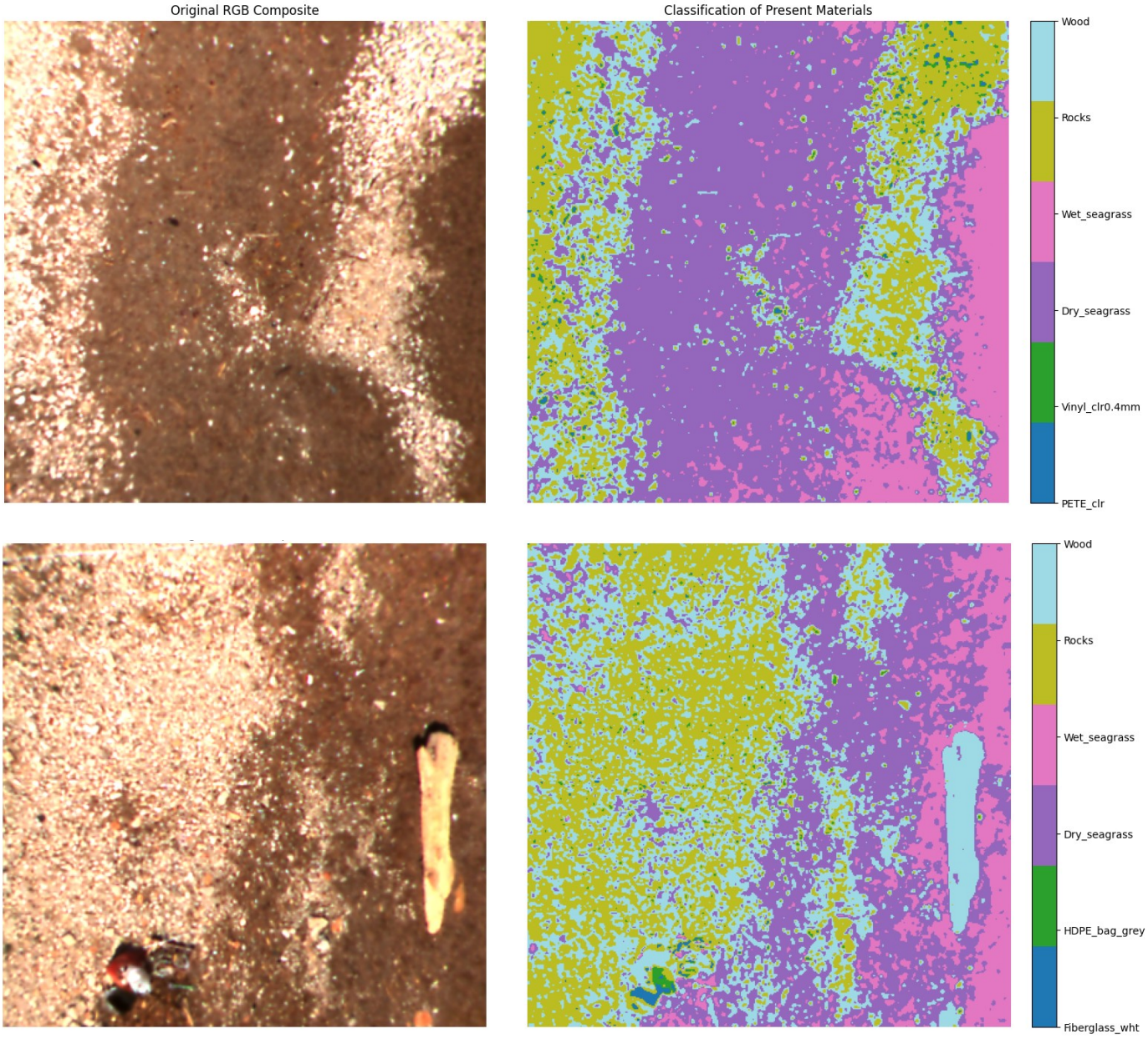


Figure 18: Original RGB images from the drone (left) compared with the SAM classification (right) of Plot 1 (up) and Plot 2 (down) at 10 m of height and 1,71 cm of spatial resolution.

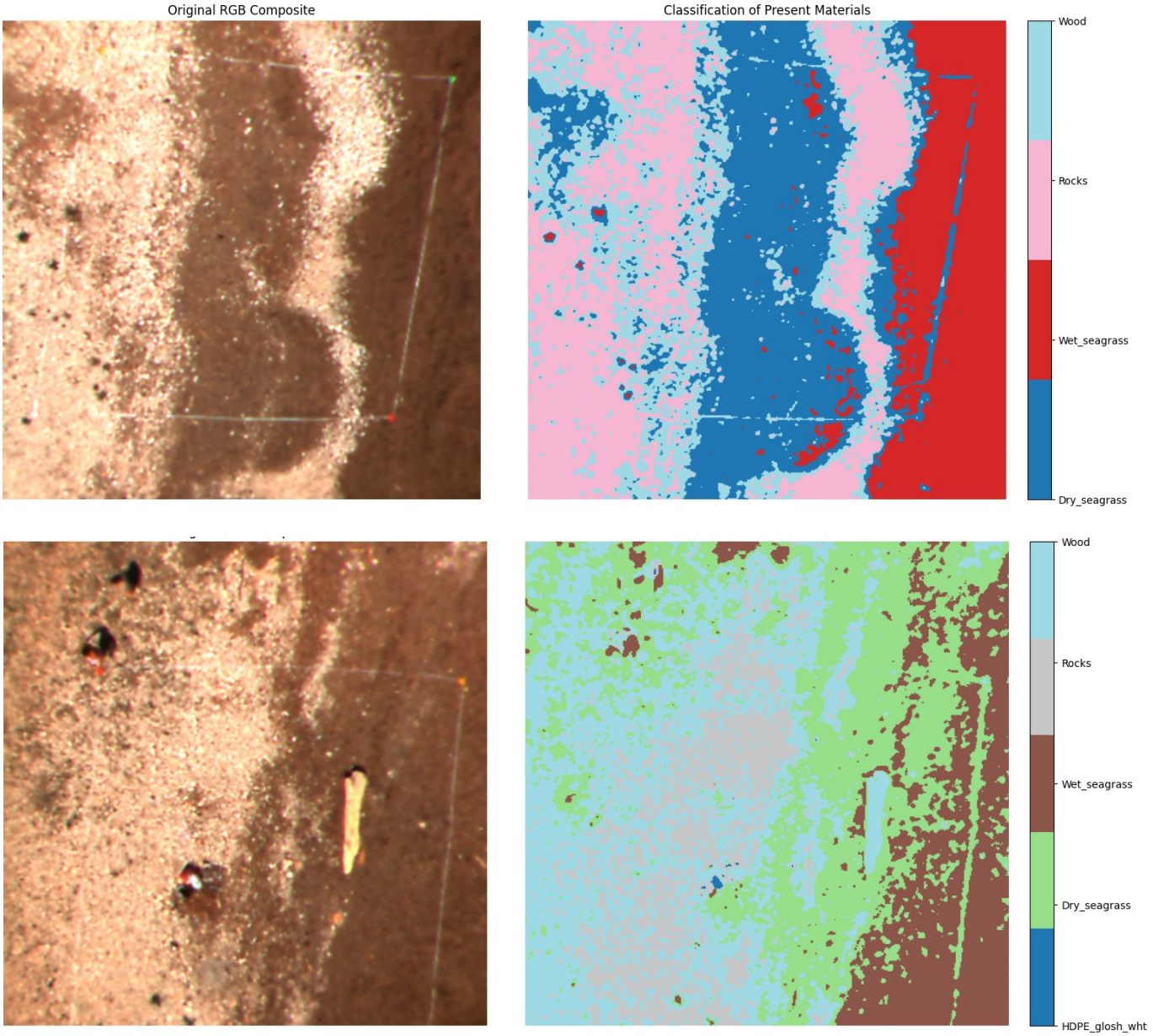


Figure 19: Original RGB images from the drone (left) compared with the SAM classification (right) of Plot 1 (up) and Plot 2 (down) at 20 m of height and 3,42 cm of spatial resolution.

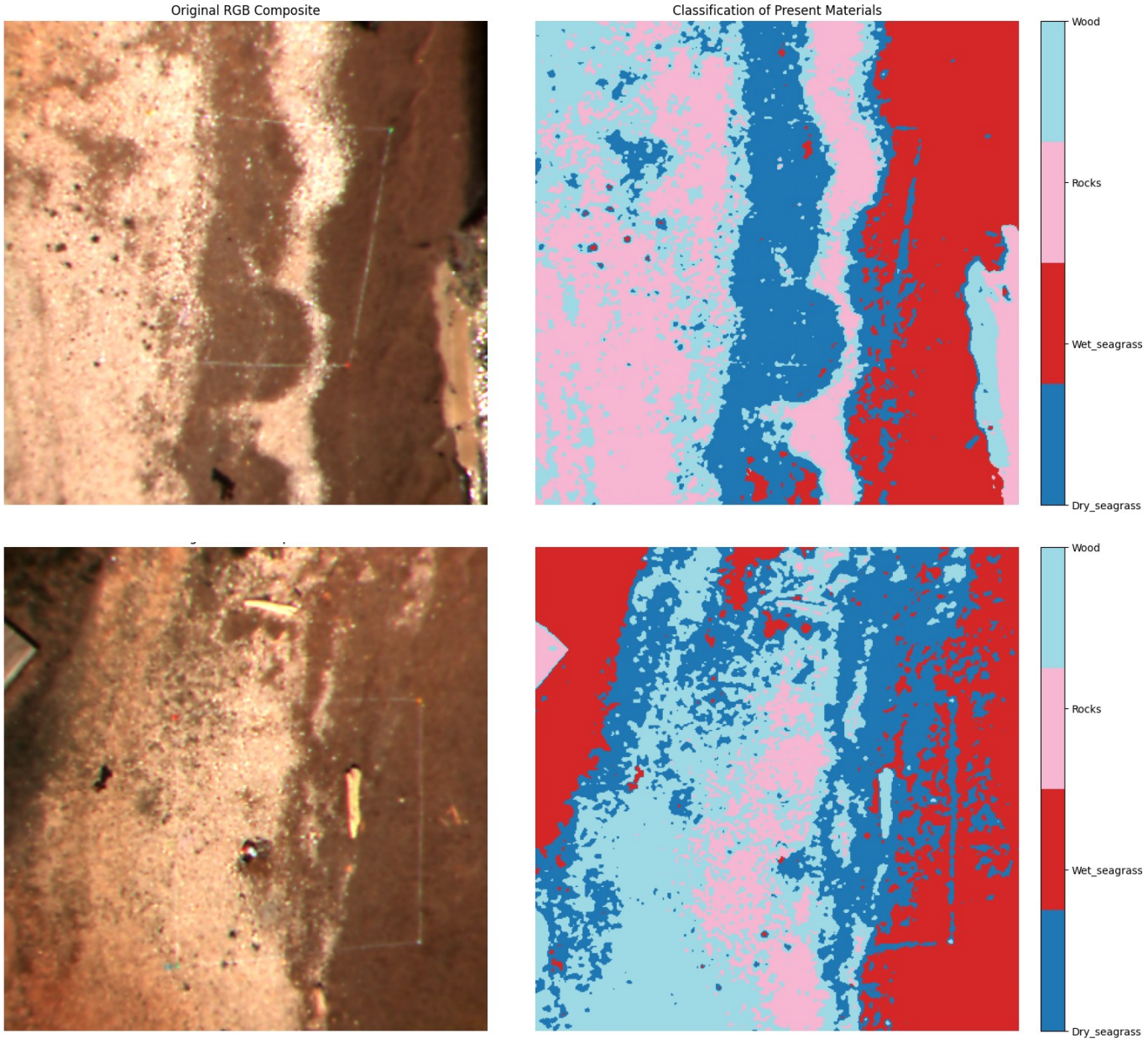


Figure 20: Original RGB images from the drone (left) compared with the SAM classification (right) of Plot 1 (up) and Plot 2 (down) at 30 m of height and 5,12 cm of spatial resolution.

4. Discussion and Conclusion

The findings from this study provide a comprehensive look into the potential and limitations of using both satellite and drone-based remote sensing for environmental waste detection. The results underscore a central challenge: there is no single, universally effective methodology. The choice of sensor and analytical approach must be a careful trade-off between image resolution, spatial and temporal scale, and the specific characteristics of the waste being targeted. With regard to the coastal waters analysis, the Floating Debris Index (FDI) applied to Sentinel-2 imagery demonstrated the potential to detect floating objects over a wide area and a long-time span. However, the study on our pilot areas did not yield a sufficient amount of detected potential plastic debris for any meaningful statistical analysis. This is primarily due to the spatial resolution of Sentinel-2 (10x10 meters), which is ill-suited for identifying small, scattered marine litter. Instead, the FDI primarily detected large floating objects such as boats, which can easily fill an entire pixel, while smaller pieces of debris remained invisible. Furthermore, the FDI detects all types of floating debris, including seafoam, seagrass, and other natural materials, which complicate the confirmation of plastics and require careful, often ambiguous interpretation. It is important to note that existing studies in the literature often use the FDI on a single or a few images to validate its feasibility with artificial targets (Biermann et al., 2020; Themistocleous et al., 2020; Pathira Arachchilage et al., 2025), rather than for long-term mapping. This highlights that a standardized methodology for long-term, wide-scale marine litter mapping is a complex task still in its early stages of development.

For the terrestrial analyses, the trade-off between image resolution and spatial-temporal extent was the main constraint. While satellite images from missions like Sentinel-2 allow for long-term and wide-scale environmental monitoring, their coarse resolution sets a hard limit on the detection of minor waste accumulations and isolated objects. Conversely, using very high-resolution images to overcome this limitation would drastically increase computational effort and data storage requirements (Fraternali et al., 2024). The use of drones emerged as a valuable option for addressing the limits of satellite data, as they provide high-resolution images capable of detecting even minor waste accumulations. However, drone-based surveys also have their own significant limitations. Their lower spatial extent necessitates continuous field surveys and active data acquisition, which is time-consuming and labor-intensive. Furthermore, meteorological conditions are a major constraint, as cloud cover and the solar incidence angle can significantly influence the spectral response and thus the uniformity of the acquired data. Standardized images, essential for comparative analysis, require acquisition under ideal conditions, such as a completely cloudless sky at noon. The hyperspectral data obtained from the drone survey provided a valuable foundation for developing a classification model. The results confirmed that plastic color is a key feature influencing the spectral response, but other, more complex properties, such as polymer composition, are also reflected in the NIR and SWIR spectra (Zhou et al., 2022; Olyaei et al., 2024). However, the performance of the Random Forest classification models was not entirely satisfactory, primarily due to the low number of training pixels for the waste classes (as seen in Table 2). The limited amount of waste found on the beach, combined with the difficult identification of waste pixels, severely restricted the model's ability to learn and accurately classify different waste types. This aligns with a core principle of machine learning, where model accuracy is strictly related to the amount and balance of training data (Huang & Bardossy, 2020; Kim et al., 2022; Rodrguez-Belenguer et al., 2025).

The different approach adopted for the SAM classification application confirmed the importance of high spatial resolution and waste dimensions. In this case, another key aspect is the availability of wide and comprehensive reference spectral data, which represents the basics for a correct interpretation of the materials found in the scene, but this is still a very difficult achievement due to the large variability of anthropogenic materials. Overall, the tool provides a reproducible workflow for hyperspectral analysis without the need for proprietary software. The application represents a prototype of a handy tool, which can be useful for the identification of waste using drone images or very high-resolution satellite images. Further refinement is still required, such as expanding the reference spectral library and testing the application with higher spatial resolution images; these improvements are expected to increase both the reliability and the applicability of the tool. Although the application was specifically designed for waste detection in natural environments, the use of alternative reference spectra could also make it suitable for geological mapping, vegetation studies, and, more generally, for any context in which the identification of surface materials from spectral information is required.

In conclusion, this study has laid the groundwork for developing a methodology for environmental waste detection using hyperspectral drone imagery, a tool with immense potential for identifying waste in hard-to-reach areas. We also analyzed the potential and limits of free satellite images, which, while inadequate for detecting minor accumulations, remain useful for identifying wider deposits such as illegal landfills. Given the uncertainties and exploratory nature of the analyses performed to date, it is important to note that the database of waste accumulation sites presented in Deliverable D.1.9.2 relies primarily on robust field observations and data retrieved from online datasets.

Reference List

Anne, N. J. P., Abd-Elrahman, A. H., Lewis, D. B. & Hewitt, N. A. Modeling soil parameters using hyperspectral image reflectance in subtropical coastal wetlands. Int. J. Appl. Earth Obs. Geoinformation 33, 47–56 (2014).

Arachchilage, K. R. L. P., Tang, D., Yu, J. & Wang, S. A Preliminary Analysis towards Detecting Floating Marine Macro Plastics Using an Index Developed for Sentinel 2 ACOLITE and Sen2Cor Images. J. Geospatial Surv. 2, (2022).

Aasen, H., Honkavaara, E., Lucieer, A. & Zarco-Tejada, P. J. Quantitative Remote Sensing at Ultra-High Resolution with UAV Spectroscopy: A Review of Sensor Technology, Measurement Procedures, and Data Correction Workflows. Remote Sens. 10, 1091 (2018).

Baba, A., Kavdir, Y. & Deniz, O. The impact of an open waste disposal site on soil and groundwater pollution. Int. J. Environ. Pollut. 22, 676–687 (2004).

Balsi, M., Esposito, S. & Moroni, M. Hyperspectral characterization of marine plastic litters. in 2018 IEEE International Workshop on Metrology for the Sea; Learning to Measure Sea Health Parameters (MetroSea) 28–32 (2018). doi:10.1109/MetroSea.2018.8657875.

Bansod, B., Singh, R. & Thakur, R. Analysis of water quality parameters by hyperspectral imaging in Ganges River. Spat. Inf. Res. 26, 203–211 (2018).

Biermann, L., Clewley, D., Martinez-Vicente, V. & Topouzelis, K. Finding Plastic Patches in Coastal Waters using Optical Satellite Data. Sci. Rep. 10, 5364 (2020).

Birky, A. K. NDVI and a simple model of deciduous forest seasonal dynamics. Ecol. Model. 143, 43–58 (2001).

Bonifazi, G., Gasbarrone, R. & Serranti, S. Detecting contaminants in post-consumer plastic packaging waste by a NIR hyperspectral imaging-based cascade detection approach. (2021).

Chang, C.-I. Hyperspectral Data Processing: Algorithm Design and Analysis. (John Wiley & Sons, 2013).

Damayanti, A. D., Hanami, Z. A., Hirose, K., Ainun, S. & Putra, R. D. Potential Marine Plastic Debris Detection using Sentinel-2 Multi-Spectral Instrument (MSI). IOP Conf. Ser. Earth Environ. Sci. 1117, 012054 (2022).

Dugin, S., Sybirtseva, O., Golubov, S., & Dorofey, Y. (2019). Verification of multispectral data processing for the Sentinel-2A bands, field ASD FieldSpec® 3FR and UAV with the DJI STS-VIS . Ukrainian Journal of Remote Sensing, (21), 29–39. https://doi.org/10.36023/ujrs.2019.21.147

Fraternali, P., Morandini, L. & Herrera González, S. L. Solid waste detection, monitoring and mapping in remote sensing images: A survey. Waste Manag. 189, 88–102 (2024).

Harris, P. J. Water quality impacts from on-site waste disposal systems to coastal areas through groundwater discharge. Environ. Geol. 26, 262–268 (1995).

Huang, Y. & Bardossy, A. Impacts of Data Quantity and Quality on Model Calibration: Implications for Model Parameterization in Data-Scarce Catchments. Water 12, 2352 (2020).

Jay, S., Lawrence, D. R., Repasky, D. K. & Keith, C. INVASIVE SPECIES MAPPING USING LOW COST HYPERSPECTRAL IMAGERY. (2009).

Kah, M., Levy, L. & Brown, C. Potential for Effects of Land Contamination on Human Health. 2. The Case of Waste Disposal Sites. J. Toxicol. Environ. Health Part B 15, 441–467 (2012).

Karakuş, O. On advances, challenges and potentials of remote sensing image analysis in marine debris and suspected plastics monitoring. Front. Remote Sens. 4, (2023).

Kim, C., Jeong, J. & Choi, J. Effects of Class Imbalance and Data Scarcity on the Performance of Binary Classification Machine Learning Models Developed Based on ToxCast/Tox21 Assay Data. Chem. Res. Toxicol. 35, 2219–2226 (2022).

Kokaly, R.F., Clark, R.N., Swayze, G.A., Livo, K.E., Hoefen, T.M., Pearson, N.C., Wise, R.A., Benzel, W.M., Lowers, H.A., Driscoll, R.L., and Klein, A.J., 2017, USGS Spectral Library Version 7 Data: U.S. Geological Survey data release, https://dx.doi.org/10.5066/F7RR1WDJ.

Kraśniewski, J., Dąbała, Ł. & Lewandowski, M. Hyperspectral Imaging for Analysis and Classification of Plastic Waste. in 2020 25th International Conference on Pattern Recognition (ICPR) 4805–4812 (2021). doi:10.1109/ICPR48806.2021.9412737.

Laurin, G. V. et al. Biodiversity Mapping in a Tropical West African Forest with Airborne Hyperspectral Data. PLOS ONE 9, e97910 (2014).

Marques, M. Stormwater runoff pollution at waste management sites. Urban Water J. 4, 173–181 (2007).

Mazanov, G. et al. Hyperspectral Data Driven Solid Waste Classification. IEEE Access 13, 46659–46672 (2025).

McFEETERS, S. K. The use of the Normalized Difference Water Index (NDWI) in the delineation of open water features. Int. J. Remote Sens. 17, 1425–1432 (1996).

Moshtaghi, M., Knaeps, E., Sterckx, S., Garaba, S. & Meire, D. Spectral reflectance of marine macroplastics in the VNIR and SWIR measured in a controlled environment. Sci. Rep. 11, 5436 (2021).

Nguyen, C. T., Chidthaisong, A., Kieu Diem, P. & Huo, L.-Z. A Modified Bare Soil Index to Identify Bare Land Features during Agricultural Fallow-Period in Southeast Asia Using Landsat 8. Land 10, 231 (2021).

Olyaei, M., Ebtehaj, A. & Ellis, C. R. A Hyperspectral Reflectance Database of Plastic Debris with Different Fractional Abundance in River Systems. Sci. Data 11, 1253 (2024).

Park, J.-J. et al. Hazardous Noxious Substance Detection Based on Ground Experiment and Hyperspectral Remote Sensing. Remote Sens. 13, 318 (2021).

Pathira Arachchilage, K. R. L., Tang, D. & Wang, S. Detection of floating marine macro plastics using a new index with remote sensing data. J. Oceanol. Limnol. (2025) doi:10.1007/s00343-024-3152-7.

Rajkumar, A., Sziranyi, T. & Majdik, A. DETECTING LANDFILLS USING MULTI-SPECTRAL SATELLITE IMAGES AND DEEP LEARNING METHODS. (2022).

Rodríguez-Belenguer, P., Beser-Robles, M., Marfil-Trujillo, M., Cerdá Alberich, L. & Martí-Bonmatí, L. The Challenge of Data Scarcity and Imbalanced Classes in Radiomics Performance. SSRN Scholarly Paper at https://doi.org/10.2139/ssrn.5281759 (2025).

Stuart, M. B., McGonigle, A. J. S. & Willmott, J. R. Hyperspectral Imaging in Environmental Monitoring: A Review of Recent Developments and Technological Advances in Compact Field Deployable Systems. Sensors 19, 3071 (2019).

Themistocleous, K., Papoutsa, C., Michaelides, S. & Hadjimitsis, D. Investigating Detection of Floating Plastic Litter from Space Using Sentinel-2 Imagery. Remote Sens. 12, 2648 (2020).

Topouzelis, K., Papakonstantinou, A. & Garaba, S. P. Detection of floating plastics from satellite and unmanned aerial systems (Plastic Litter Project 2018). Int. J. Appl. Earth Obs. Geoinformation 79, 175–183 (2019).

Zhou, S. et al. Identifying distinct plastics in hyperspectral experimental lab-, aircraft-, and satellite data using machine/deep learning methods trained with synthetically mixed spectral data. Remote Sens. Environ. 281, 113263 (2022).